Diplomarbeit

Brain iron deposits in Parkinson's disease/ Zerebrale Eisenablagerung bei Morbus Parkinson

eingereicht von

Sebastian Franthal

zur Erlangung des akademischen Grades

Doktor der gesamten Heilkunde

(Dr. med. univ.)

an der

Medizinischen Universität Graz

ausgeführt an der

Universitätsklinik für Neurologie

unter der Anleitung von

Ass.-Prof.in Priv.-Doz.in Dr.in med.univ. Petra Schwingenschuh

sowie

Dr.in med.univ. Nina Homayoon

Graz, 24.05.2016

Eidesstattliche Erklärung

Ich erkläre ehrenwörtlich, dass ich die vorliegende Arbeit selbstständig und ohne fremde Hilfe verfasst habe, andere als die angegebenen Quellen nicht verwendet habe und die den benutzten Quellen wörtlich oder inhaltlich entnommenen Stellen als solche kenntlich gemacht habe.

Graz, am 24.05.2016 *Sebastian Franthal, eh*

Danksagungen

An dieser Stelle möchte ich mich bei allen bedanken, die mir die Absolvierung meines Studiums ermöglicht haben und mich bei der Erstellung meiner Diplomarbeit unterstützt haben.

Der Dank richtet sich an die Medizinische Universität Graz und an alle Lehrenden, die mich auf dem Weg meiner Ausbildung begleitet haben.
Besonders hervorheben möchte ich meine Diplomarbeitsbetreuerinnen und -betreuer Petra Schwingenschuh, Nina Homayoon und Stephan Seiler, die mir immer mit Rat und Tat zur Seite gestanden sind und auf deren Unterstützung ich mich verlassen konnte.
Großer Dank geht auch an Lukas Pirpamer und Christian Langkammer, die mich in technischen Fragen und mit der technischen Auswertung der MR-Daten tatkräftig unterstütz haben.
Bedanken möchte ich mich nicht zuletzt beim gesamten Team der Neurogeriatrie für die überaus freundliche Aufnahme und natürlich auch bei allen Patientinnen und Patienten für die Bereitschaft einen Beitrag zur Wissenschaft zu leisten.

Ganz besonderer Dank gilt natürlich auch an dieser Stelle meinen Eltern und meiner Familie, die mir mein Studium ermöglicht haben und mich immer großartig unterstütz haben.

Schlussendlich möchte ich meinen Dank auch an die Republik Österreich richten, die mir hochwertige Schulbildung und ein Hochschulstudium meiner Wahl ermöglicht und finanziert hat.

Abstract

Objective

To describe longitudinal evolution of brain iron deposits in Parkinson's disease (PD) over a period of two years, measured by R2* weighted MRI, and compare the findings to non-degenerative tremor syndromes.

Materials and Methods

32 PD patients and 15 patients suffering from non-degenerative tremor syndromes (i.e. essential or dystonic tremor) were drawn from the longitudinal registry on movement disorders in Graz (PROMOVE). All subjects underwent detailed clinical examination and 3T MRI scans at baseline and after a follow-up period of two years. R2* was reconstructed from gradient echo sequences, acquired with the identical spoiled 3D FLASH sequence, with 6 equally spaced echoes.

Results

During the two year evolution of PD, R2* increased significantly in substantia nigra and tended to correlate inversely with increase in L-dopa equivalent dose. R2* values contralateral to the clinically more affected side did not show stronger increase and there was no significant difference between tremor dominant and non-tremor dominant motor phenotype in PD. We found no significant difference between PD and the non-degenerative tremor group in R2* increase. However, R2* values in substantia nigra were significantly higher in PD compared to the non-degenerative tremor group at baseline and follow-up, which is a novel finding.

Conclusions

There is a trend for stronger longitudinal increase of iron concentration in substantia nigra in PD compared to our control group and a possible protective effect of levodopa on iron deposits in substantia nigra in PD. Further studies including higher case-numbers and more sensitive techniques are needed. R2* might be useful as a cost-effective, non-invasive biomarker in differential diagnosis of tremor syndromes.

Zusammenfassung

Ziele

Die longitudinale Entwicklung von zerebralen Eisenablagerungen bei Morbus Parkinson (MP) über einen Zeitraum von zwei Jahren, gemessen mit R2* gewichtetem MR, zu beschreiben und die Ergebnisse mit nichtdegenerativen Tremor-Syndromen zu vergleichen.

Methoden

32 MP Patientinnen und Patienten und 15 Kontrollen mit essentiellem oder dystonem Tremor, aus der longitudinalen Datenbank für Bewegungsstörungen in Graz (PROMOVE), wurden einbezogen. Alle Personen unterzogen sich detaillierten klinischen Untersuchungen und 3T-MR Scans zur Baseline und nach einen Follow-up Zeitraum von zwei Jahren. R2* wurde aus Gradienten-Echo-Sequenzen, aufgenommen mit einer gleichmäßig verzögerten 3D FLASH Sequenz, mit 6 abstandsgleichen Echos, rekonstruiert.

Ergebnisse

Während des zweijährigen Fortschreitens von MP nahm R2* in der Substantia nigra signifikant zu und neigte zu einer inversen Korrelation mit dem Anstieg der L-Dopa Äquivalenz-Dosis. R2* Werte kontralateral zur klinisch stärker betroffenen Seite zeigten keine stärkere Zunahme und es gab keinen signifikanten Unterschied zwischen Tremor- und nicht-Tremor-dominantem Motor-Phänotyp in MP. Es konnte kein signifikanter Unterschied betreffend R2* Zunahme zwischen MP und Kontrollen gefunden werden. Allerdings zeigte diese Studie erstmals signifikant höhere R2* Werte in der Substantia nigra zur Baseline und zum Follow-up bei MP im Vergleich zu nichtdegenerativen Tremor-Syndromen.

Schlussfolgerungen

Es zeigt sich ein Trend für stärkere longitudinale Zunahme der Eisenkonzentration in der Substantia nigra in MP verglichen mit Kontrollen und ein potentiell protektiver Effekt von Levo-Dopa auf Eisenablagerungen in der Substantia nigra bei MP. Allerdings müssen diese Ergebnisse noch durch höhere Fallzahlen und sensitivere Methoden bestätigt werden. R2* könnte ein kosten-effizienter, nicht invasiver Biomarker in der Differentialdiagnose von Tremor-Syndromen sein.

Table of Contents

List of Abbreviations

CN	.....	Caudate nucleus
CO	.....	Cortex
CONT	.....	Control group
DBS	.....	Deep brain stimulation
eGP	.....	External pallidum
FTM	.....	Fahn-Tolosa-Marin tremor rating scale
iGP	.....	Internal pallidum
IPS	.....	Idiopathic Parkinson Syndrome
LED	.....	Levodopa equivalent dose
MMSE	.....	Mini Mental Status Examination
MRI	.....	Magnetic Resonance Imaging
NMS	.....	Nonmotor Symptoms Questionnaire
NTD	.....	Non-tremor-dominant
PD	.....	Parkinson’s disease
QSM	.....	Quantitative susceptibility mapping
ROI	.....	Region of interest
SD	.....	Standard-deviation
SN	.....	Substantia nigra
SNc	.....	Substantia nigra pars compacta
SNr	.....	Substantia nigra pars reticulata
STM	.....	Striatum
STN	.....	Subthalamic nucleus
SWI	.....	Susceptibility weighted imaging
TCS	.....	Transcranial sonography
TD	.....	Tremor-dominant
TH	.....	Thalamus
TMT	.....	Trail Making Test

List of Figures

List of Tables

1 Introduction

1.1 Parkinson's Disease

Parkinson's disease (PD) is a degenerative movement disorder caused by loss of dopaminergic neurons in the substantia nigra. Its main symptoms are bradykinesia, resting tremor, rigidity, and postural instability.

1.1.1 Epidemiology

The typical age of onset of idiopathic PD is between 45 and 70 years with a peak in the sixth decade. Idiopathic PD is observed across all countries, all ethnic groups, and all socioeconomic classes. In North American and European countries there is about one percent of the population over 65 suffering from PD (1).

Studies done in several European countries estimate prevalence of PD 108 to 257 per 100000 (2). It increases with age (41 per 100000 in individuals 40 to 49 years up to 1903 per 100000 in individuals over age 80, (3)) and occurs more frequently in men (559 per 100000 in males relative to 358 per 100000 in females, age 50-89, (4)).

PD incidence rates are 11 to 19 per 100000 per year (1,2).

1.1.2 Pathophysiology

The definite cause for PD is unknown. There is evidence that genetic in combination with environmental factors trigger the progressive loss of pigmented cells in the substantia nigra and other pigmented nuclei. Macroscopically the substantia nigra turns pale; microscopically the pigmented nuclei show a marked depletion of cells and replacement gliosis as well as reduced quantities of melanin in some of the remaining cells (1,5-17). Another characteristic histological sign in patients with idiopathic PD are eosinophilic cytoplasmatic inclusions, surrounded by a faint halo, which are called Lewy bodies. These Lewy bodies mainly consist of α-synuclein filaments and other less specific proteins like ubiquitin and tau in lower concentrations. α-synuclein in its unfolded form is a physiologically existing synaptic and nuclear protein, but in higher concentrations it aggregates and has neurotoxic effects. A model published by Eriksen et al. suggests that point mutations as well as functional duplications of the α-synuclein gene lead to excessive intracellular accumulation of α-synuclein, resulting in spontaneous

oligomerisation of the protein. Moreover mutations in Parkin and UCH-L1 genes as well as the mutated α-synuclein itself inhibit the normal removal of synuclein by the proteasoms. Provoked by these processes and increased by heat shock proteins and - for PD especially relevant - dopamine, synuclein polymerises to form neurotoxic protofibrils, which lead to the formation of Lewy bodies (1,7).

On the other hand, the extrapyramidal cerebral functional circuits necessary to enable correct movement of the human body and their dysfunction in PD are well known. There are two main pathways which inhibit neurons in the ventrolateral and ventroanterior nuclei of the thalamus resulting in reduced thalamocortical input to the precentral motor fields and therefore inhibit voluntary motor output (Figure 1). This inhibition is enhanced in PD leading to the typical symptoms (18).

The *direct* pathway is activated on the one hand by glutaminergic projections from the sensorimotor cortex and on the other hand dopaminergic (D1 excitatory) projections from the substantia nigra pars compacta, which activate inhibitory gamma-aminobutyric acid (GABA) projections from the striatum to the internal (medial) pallidum and the substantia nigra pars reticulata. These two areas are believed to act as one entity which projects via GABA-containing neurons to the thalamus and inhibits the thalamocortical projections. As a result this pathway enhances voluntary movement (18).

Mathematically thought, excitatory influence can be written as “+” and inhibition as “-“. The direct pathway can be summarised in the following equation, resulting in excitatory influence: [SNc/CO(+)STM(-)iGP/SNr(-)TH(+)CO=(+)]

The *indirect* pathway arises from striatal neurons, which are inhibited by dopaminergic (D2) nigral (pas compacta) - striatal projections. These striatal GABA-containing neurons have an inhibiting influence on the external (lateral) pallidum, which inhibits the subthalamic nucleus. The subthalamic nucleus on the other hand, activates (by glutaminergic projections) the “internal pallidum – substantia nigra pars reticulata entity” which inhibits the thalamic nuclei. As a result this pathway again enhances voluntary movement (18).

Indirect pathway: [SNc(-)STM(-)eGP(-)STN(+)iGP/SNr(-)TH(+)CO=(+)]

In PD the activity of the substantia nigra pars compacta is reduced, namely there is less dopaminergic influence on the striatum. As a result the pathways have the opposite effect and the cortical motor output is reduced (Figure 2).

On the one hand, because of the lower D1 excitatory influence on the striatum the activity of the direct pathway is decreased. This leads to a decreased striatal inhibition of the “internal pallidum – substantia nigra pars reticulata entity” which in turn causes an increased inhibition of the thalamic nuclei.

Direct pathway: [**-**SNc/CO(+)STM(-)iGP/SNr(**-**)TH(+)CO=(**-**)]

On the other hand, because of the lower D2 inhibitory influence on the striatum the activity of the indirect pathway is increased. The enhanced inhibitory striatal-palladinal projections cause lower palladinal inhibition of the subthalamic nucleus, which in turn leads to an enhanced inhibition of the thalamic nuclei by the “internal pallidum – substantia nigra pars reticulata entity”.

Indirect pathway: [**-**SNc(-)STM(**-**)eGP(-)STN(**+**)iGP/SNr(**-**)TH(+)CO=(**-**)]

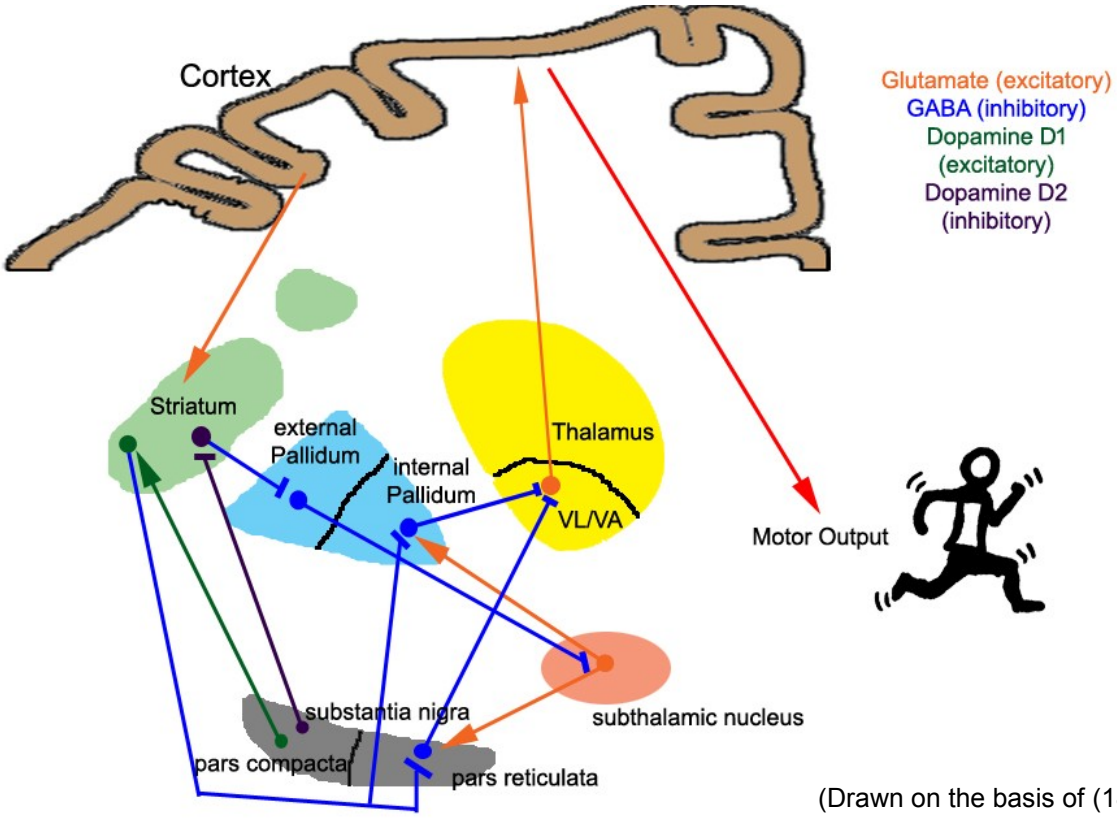

(Drawn on the basis of (18,140))

Figure 1. Normal neurotransmitter pathways and their effects in the cortical-basal ganglia-thalamic circuits

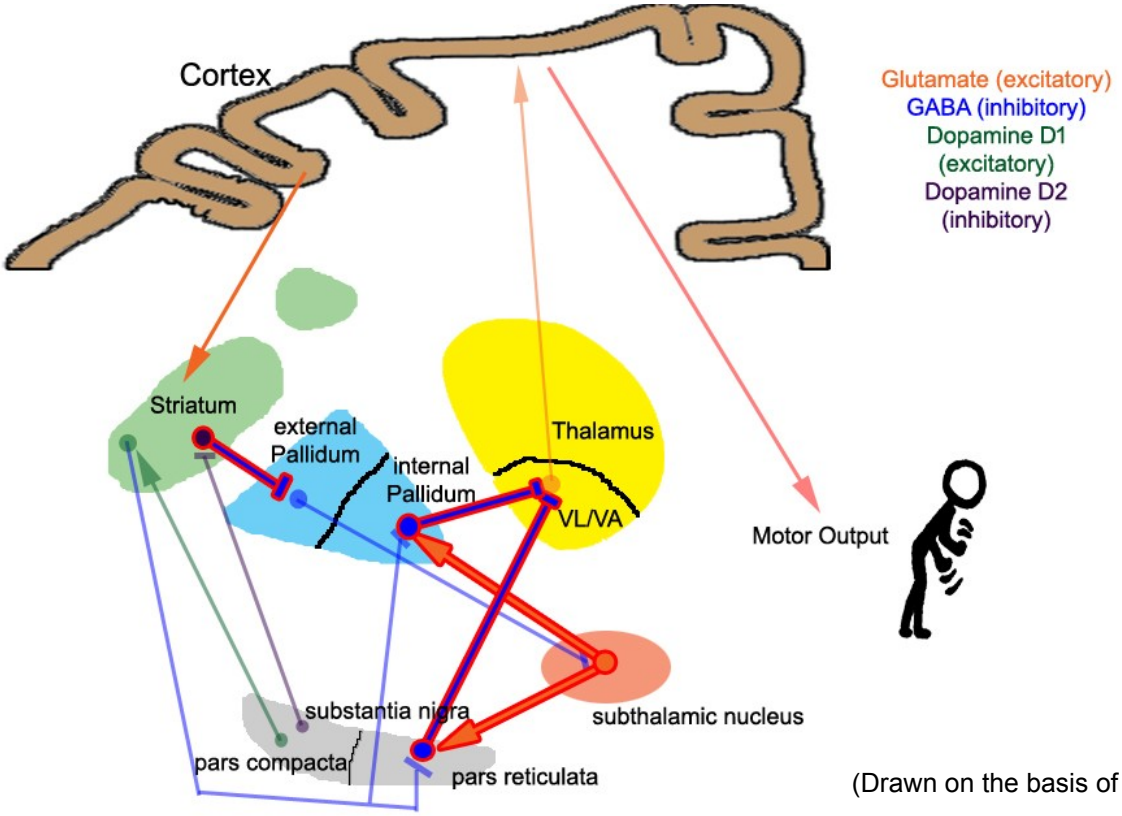

(Drawn on the basis of (18,140))

Figure 2. Neurotransmitter pathways and their effects in the cortical-basal ganglia-thalamic circuits in PD

1.1.3 Clinical Symptoms and Progression

1.1.3.1 Symptoms

1.1.3.1.1 Motor Symptoms

The cardinal symptoms of PD are hypo- and/or bradykinesia, resting tremor, rigidity, and postural instability.

Bradykinesia describes a general slowness of voluntary movement. The reaction-time, as well as the time between beginning and completion of a movement is increased. The frequent habitual movements, like putting the hands to the face, folding arms or swinging of the arms while walking are absent or reduced. A reduced blink-rate (10-20/min to 5-10/min in PD) and a slight widening of the palpebral fissures may occur. Drooling occurs because saliva is not swallowed as quickly as produced. The face is expressionless ("masked face" or hypomimia) and the speech is rapid, mumbling and monotonic (1,18).
Hypokinesia is a reduction in spontaneous movements of an affected part of the body and failure to engage it freely in the natural actions of the body. In contrast to paralysis, strength is not altered (1,18).

Resting tremor is a coarse, rhythmic tremor with a frequency of 3 to 5 Hz. In PD it is usually asymmetrically localised in one or both hands and forearms (flexion-extension or abduction-adduction of the fingers or the hand as well as pronation-supination of the hand and the forearm) and less frequently in the feet, jaw, lips, or tongue. It occurs in a repose-state and on the one hand can be temporary suppressed by voluntary movement and on the other hand its amplitude is increased by emotional stress (19).

Rigidity describes a state of altered muscle tone in which the muscles are continuously firm and tense with a low threshold for involuntary sustained muscle contraction, which is present during most of the waking state. In contrast to spasticity, the increased resistance on passive movement that characterises rigidity is not preceded by an initial free interval but has an even or uniform quality

throughout the whole movement like bending a lead pipe. The tendon reflexes are not enhanced and the rigid limb does not resume its original position, as it happens in spasticity. Rigidity concerns all muscle groups, but it tends to be more prominent in flexors (18).

Postural instability shows as stoop posture and axial instability, which is due to impairment of anticipatory and compensatory righting reflexes. A gentle push may cause a patient to fall or start an involuntary series of small corrective steps (18).

Prevalence of Motor Symptoms

Hoehn and Yahr described the prevalence of motor symptoms in a cohort of 183 patients with PD in the initial state. Their findings are summarised in Table 1 (20).

Prevalence of motor symptoms in PD initial state	
Symptom	**Prevalence**
Tremor	70.5%
Gait disturbance	11.5%
Stiffness	9.8%
Slowness	9.8%
Loss of dexterity	7.7%
Handwriting disturbance	4.9%
Speech disturbance	3.8%
General fatigue, muscle weakness	2.7%
Loss of arm swing	1.6%
Facial masking	1.6%
Dysphagia	0.5%

Table 1. Prevalence of motor symptoms in PD initial state adapted from Hoehn and Yahr 1967 (20)

1.1.3.1.2 Non-motor Symptoms

Non-motor parkinsonian symptoms include paresthetic and other sensory complaints, reduced smelling, drooling, seborrhoea, excessive sweating, constipation, abdominal pains and cramps, erectile dysfunction, joint aches as well as major cognitive disorder (1). Non-motor symptoms like reduced smelling, constipation, cardiac sympathetic denervation or REM-sleep behaviour disorder on the one hand occur very early in PD (so called “pre-motor-phase”) or on the other hand are late-symptoms like dementia (21).

Prevalence of Non-motor Symptoms

Table 2 and Table 3 summarise prevalence rates of non-motor symptoms in PD. Moreover there are upward-trends in the occurrence of dribbling, impaired taste/smelling, constipation, urinary urgency, nocturia, hallucinations and acting out during dreams with the increase of age at onset and older age at onset is an independent risk factor for dementia (22). A meta-analysis suggests that 24 to 31% of PD patients have dementia, and that 3 to 4% of the dementia in the population would be due to PD-Dementia (23).

Prevalence of non-motor symptoms in PD initial state	
Symptom	**Prevalence (%)**
Muscle pain, cramps, aching	8.2
Depression, nervousness or psychiatric disturbance	4.4
Drooling	1.6
Paresthesia	0.5
Table 2. Prevalence of non-motor symptoms in PD initial state adapted from Hoehn and Yahr 1967 (20)	

Prevalence of non-motor symptoms in PD	
Symptom	**Prevalence (%)**
Cognitive impairment	46.9
Hallucinations, psychosis	11.7
Depressed mood	61.2
Anxious mood	55.6
Apathy	32.4
Dopamine dysregulation syndrome	12.9
Sleep problems	62.9
Daytime sleepiness	62.9
Pain and other sensations	57.8
Urinary problems	63.8
Constipation problems	69.8
Light headedness	35.7
Fatigue	65.7
Table 3. Prevalence of non-motor symptoms in PD adapted from Martinez-Martin et al. 2015 (24)	

1.1.3.2 Diagnostic Criteria and Important Rating Scales

PD is diagnosed clinically and can by supported by imaging techniques and verified by post mortem histological analysis of the basal ganglia. The UK Brain Bank Criteria are the most accepted diagnostic criteria for PD and are summarised in Table 4 (25).

The UPDRS (Unified Parkinson's Disease Rating Scale) and its revision modified by the Movement Disorder Society (MDS-UPDRS) are the gold-standard in clinical

assessment of PD. The scale is divided in four sub scales: I: Non-motor Experiences of Daily Living; II: Motor Experiences of Daily Living; III: Motor Examination; IV: Motor Complications. It considers all in all 65 items, each question has five responses that are linked to commonly accepted clinical terms: 0: normal, 1: slight, 2: mild, 3: moderate and 4: severe. Table 5 lists the items assessed by MDS-UPDRS. Moreover the patient's medication, influence of dyskinesias on the assessment, Hoehn and Yahr state and the person who answers (patient or caregiver) is taken into consideration (26).

PD progression is commonly described by the Hoehn and Yahr Scale. This staging tool categorises patients and disease progression on the basis of the degree of clinical disability. The Hoehn and Yahr stages are described in Table 6 (20).

UK Parkinson's Disease Society Brain Bank clinical diagnostic criteria

Step 1 Diagnosis of Parkinsonian syndrome
• Bradykinesia (slowness of initiation of voluntary movement with progressive reduction in speed and amplitude of repetitive actions)
• And at least one of the following:
  ○ muscular rigidity
  ○ 4-6 Hz rest tremor
  ○ Postural instability not caused by primary visual, vestibular, cerebellar, or proprioceptive dysfunction.

Step 2 Exclusion criteria for Parkinson's disease • History of repeated strokes with stepwise progression of parkinsonian features • History of repeated head injury • History of definite encephalitis • Oculogyric crises • Neuroleptic treatment at onset of symptoms • More than one affected relative • Sustained remission • Strictly unilateral features after 3 years • Supranuclear gaze palsy • Cerebellar signs • Early severe autonomic involvement • Early severe dementia with disturbances of memory, language, and praxis • Babinski sign • Presence of cerebral tumour or communicating hydrocephalus on CT scan • Negative response to large doses of levodopa (if malabsorption excluded) • MPTP exposure
Step 3 Supportive prospective positive criteria for Parkinson's disease (Three or more required for diagnosis of definite Parkinson's disease) • Unilateral onset • Rest tremor present • Progressive disorder • Persistent asymmetry affecting side of onset most • Excellent response (70-100%) to levodopa

• Severe levodopa-induced chorea • Levodopa response for 5 years or more • Clinical course of 10 years or more
Table 4. UK Parkinson's Disease Society Brain Bank clinical diagnostic criteria (25)

MDS-UPDRS			
Part I	**Part II**	**Part III**	**Part IV**
Cognitive impairment	Speech	Speech	Time spent with dyskinesia
Hallucinations and psychosis	Salivation and drooling	Facial expression	Functional impact of dyskinesias
Depressed mood	Chewing and swallowing	Rigidity of neck and four extremities	Time spent in the OFF state
Anxious mood	Eating tasks	Finger tapping	Functional impact of fluctuations
Apathy	Dressing	Hand movements	Complexity of motor fluctuations
Features of dopamine dysregulation syndrome	Hygiene	Pronation/ supination movement of hands	Painful OFF-state dystonia
Nighttime sleep problems	Handwriting	Toe tapping	
Daytime sleepiness	Doing hobbies and other activities	Leg agility	
Pain and other sensations	Turning in bed	Arising from chair	
Urinary problems	Tremor	Gait	
Constipation problems	Getting out of bed, car, or deep chair	Freezing of gait	
Lightheadedness on standing	Walking and balance	Postural stability	
Fatigue	Freezing	Posture	
		Global spontaneity of movement	
		Postural tremor of hands	
		Kinetic tremor of hands	
		Rest tremor amplitude	
		Constancy of rest tremor	
Table 5. MDS-UPDRS assessment items (26)			

Hoehn and Yahr Scale	
Stage I	Unilateral involvement only, usually with minimal or no functional impairment.
Stage II	Bilateral or midline involvement, without impairment of balance.
Stage III	First signs of impaired righting reflexes. This is evident as the patient turns or is demonstrated when he or she is pushed from standing equilibrium with the feet together and eyes closed.
Stage IV	Fully developed, severely disabling disease; the patient is still able to walk

	and stand unassisted but is markedly incapacitated.
Stage V	Confinement to bed or wheelchair unless aided.
Table 6. Hoehn and Yahr Scale (20)	

1.1.3.3 Progression

The symptoms begin slowly, characteristically starting in one limb and spreading at first to one and then to both sides. PD often starts with the speech becoming soft and monotonous, aching in the back, reduced smelling, depression, constipation and diffuse slowness of motion. As the disorder worsens, most activities of daily life are affected. Handwriting becomes small and tremulous, the voice turns into a whispering, eating and swallowing become more and more difficult, walking is reduced to a shuffle and patients frequently loose balance. Moreover patients “freeze” for instance at obstacles like door thresholds and the turning over while sleeping is reduced to a minimum. Furthermore fragments of dystonia like persistent extension or clawing of the toes or jaw clenching might occur (1). After 10 to 20 years of disease progression 40-75% of PD patients die and about 50% of those who survive require nursing home care (27).

Progression of motor symptoms

Longitudinal data from patients in placebo controlled studies during a 6- to 12-month placebo phase show an increase of 8 to 10 points for the total UPDRS and of 5 to 6 points for the motor scores alone. This progression is non-linear, slowing down with time (21,27). Longitudinal data acquired over a period of up to eight years, show an increase of UPDRS total motor scores at an annual rate of 1.5% and 3.6% in those who die during the follow-up period (28). Tremor progresses more slowly than the other cardinal symptoms, so the akinetic-rigid type has faster disease progression than the tremor-dominant type of PD (27-30).

Progression of non-motor symptoms

Table 7 shows progression of non-motor symptoms in early untreated PD patients over a period of 2 years. At baseline, nearly all patients (97.8%) stated at least one non-motor symptom, but only pains, sex difficulty as well as weight significantly increased and depression and anxiety significantly decreased (31).

The Sydney multicentre study describes the long-term progression of initially untreated PD patients over a period of 20 years. The prevalence of non-motor symptoms at the 15 and 20 year follow-up are summarised in Table 8. The rates for falls, urinary incontinence and especially dementia are significantly higher than in general population studies of people of similar age after 15 years of PD and further increase after 20 years disease duration (32,33).

The cognitive decline of patients, who develop cognitive impairment in PD, is estimated to be 2 points in the Mini Mental Status Examination per year (21) and depression score doubles in a period of 5 years (30).

	% Baseline (early untreated PD)	**% Follow-up (2 years)**	**Percentage change**	**p Value**
Dribbling	18.7	13.2	29.4	0.311
Taste/smelling	25.3	23.8	-5.9	0.653
Swallowing	10.9	12.1	+11	0.764
Vomiting	2.2	3.3	+50	0.983
Constipation	9.9	18.7	+88.8	0.092
Bowel incontinence	0	0	-	-
Bowel emptying incompleted	12.1	10.9	-9.9	0.671
Urgency	17.6	18.7	+6.2	0.852
Nocturia	16.5	7.7	-53.3	0.065
Forgetfulness, memory	16.5	20.1	+2.2	0.454
Loss of interest	27.5	18.7	-5.8	0.167
Concentrating	14.3	18.9	+32.1	0.431
Hallucinations	1.1	3.3	+200	0.623
Delusions	0	2.2	-	0.494
Sad, blues	43.9	21.1	-51.9	**0.001**
Anxiety	54.9	39.5	-28.1	**0.038**
Sex drive	0	3.3	-	0.25
Sex difficulty	6.6	17.6	+166.6	**0.039**
Dizzy	10.9	6.6	-39.4	0.294
Falling	0	0	-	-
Daytime sleepiness	3.3	4.4	+33.3	0.943
Insomnia	23.1	24.2	+4.7	0.861
Intense, vivid dreams	6.6	9.9	+50	0.419
Acting out during dreams	32.9	37.8	+14.8	0.498
Restless legs	3.3	2.2	-33.3	0.876
Pains	7.7	18.7	+142.8	**0.028**
Weight	7.7	23.1	+200	**0.004**
Swelling	14.3	13.2	-0.9	0.831
Sweating	4.4	3.3	-25	0.987
Diplopia	4.4	9.9	+125	0.246

Table 7. Frequencies and percentage change of non-motor symptoms in early PD adapted from Erro et al. 2013 (31).

Symptom	Prevalence (%)	
	15 years	**20 years**
Falls	81	87
Choking	50	48
Symptomatic orthostatic hypertension	35	48
Urinary incontinence	41	71
Depression	50	–
Hallucinosis	50	74
Dementia	48	83
Nursing home care	40	48

Table 8. Long-term progression of non-motor symptoms according to the Sydney multicentre study (Hely et al. 2005, 2008) (32,33).
Table adapted from Poewe 2009 (21)

1.1.4 Therapy

There is no curative treatment for PD and no way to stop neuro-degeneration has been found. However there are several possibilities to provide symptom-relief, based on three columns: medication, surgical and ancillary treatment.

The gold-standard in *medication* is the dopamine-precursor levodopa (L-dopa) combined with a decarboxylase inhibitor, which minimises peripheral effects and depletion. L-dopa, in contrast to the decarboxylase inhibitor, passes the blood-brain- barrier and is converted to dopamine in the remaining cell of the substantia nigra. Initially this improves the symptoms considerably, but as the disease progresses and the number of nigral neurons is further reduced as well as the receptivity to dopamine of the striatal target neurons becomes excessive, the response to L-dopa is reduced and the intake leads to dyskinesias (L-dopa long-term syndrome). COMT-inhibitors prevent L-dopa breakdown and extend its effects. An alternative, but also a supplement to L-dopa, are dopamine agonists with direct effects on striatal neurons. Drugs with positive effects in PD are also the NMDA-antagonist amantatine and monoamine-oxidase-B inhibitors, which preserve dopamine.

Nowadays ablative *surgical treatment* has been replaced by deep brain stimulation (DBS), where electrodes are stereotactically implanted in the posterior and ventral parts of the subthalamic nucleus or in the internal segment of globus pallidus. DBS primary comes into consideration for patients with L-dopa long-term syndrome or

otherwise failure of medication after a long period of treatment. It reduces PD symptoms and dopamine treatment side effects like dyskinesia.

Ancillary treatments include physical, occupational and speech therapy, exercise programs as well as mechanical therapies (1).

1.2 Correlation of Iron and Parkinson's Disease

The role of iron as a cause for PD or just one factor in a chain of pathophysiological reactions is discussed controversially. There is evidence that long-term occupational and dietary metal exposure relates to the occurrence of PD (34). Data from imaging and histological or biochemical studies showed significant higher levels of iron deposits in the substantia nigra as well as increased levels of iron in individual dopaminergic neurons of PD patients. The results for other brain regions are controversial (34-37). Biochemical findings supporting the role of iron in pathogenesis of PD are an inverse proportion of iron content SNc>SNr in PD when SNr>SNc in healthy subjects as well as a shift of Fe^{3+}:Fe^{2+} from 2:1 in normal subjects to 1:2 in patients with PD. This shift to the more toxic iron form may further support neuro-degeneration (38). However, there were also studies that did not corroborate these findings (34-37).

Metal ions as the redox-active iron can generate oxidative stress by production of ROS (reactive oxidative species), which leads to several reactions and results in inflammation and neuro-degeneration. For instance hydrogen peroxide, which is generated during normal cellular metabolism, can be converted to the extremely toxic hydroxyl radical in the presence of iron. Subsequently these free radicals may provoke cellular damage, lipid peroxidation and eventually apoptosis and cellular destruction (38).

A key process is the Fenton reaction, which biochemically describes the reaction of iron (namely ferrous iron Fe^{2+}) and hydrogen peroxide leading to lipid peroxidation, which in turn results in a loss of membrane permeability to calcium with the associated cellular toxicity:

$Fe^{2+} + H_2O_2 \rightarrow Fe^{3+} + OH + \bullet OH$

The free radicals (•OH) produce organic free radicals (R•) by taking an electron from a polyunsaturated fatty acid (RH) in the brain:

$RH + \bullet OH \rightarrow R\bullet + H_2O$

The organic free radicals react with oxygen and form organic oxygen radicals (RO2•):

$R• + O_2 \rightarrow RO_2•$

On the one hand those radicals may perpetuate damage by reacting with other lipids through a chain reaction leading to the oxidative destruction of lipids (lipid peroxidation). Or on the other hand organic oxygen radicals can steel an electron from other biological molecule (RH) and form an organic hydroperoxide (ROOH) plus another free radical to continue the cycle:

$RO_2• + RH \rightarrow ROOH + R•$ (39)

The inflammation and activation of microglial cells going along with these processes in return lead to the production of inflammatory cytokines like TNF-α which influence the iron homeostasis and increase iron intake in neuronal cells.

In PD compared to other ironstorage disorders like untreated genetic haemochromatosis or thalassaemia, relatively low amounts of iron lead to cell-degeneration and clinical symptoms. On a molecular basis dopaminergic cells seem to be more vulnerable concerning iron accumulation and oxidative stress. Dopamine is believed to be a major source of reactive oxygen species (ROS) within the nigral cells. Oxidation of dopamine by monoamine oxidase releases hydrogen peroxide, which could in turn produce more toxic hydroxyl again mediated by the action of iron (36,40).

Moreover iron seems to play a role in the formation of Lewy bodies by inducing the aggregation of α-synuclein. Iron catalyses oxidative reactions converting α-helical α-synuclein protein-conformation into β-pleated sheet conformation, which is the form of synuclein found in Lewy bodies (34,36,40).

Increased brain iron content in PD seems to be multifactorial. Possible causes include changes in iron release mechanisms across the blood–brain barrier, and dysregulation of iron homeostasis in the substantia nigra (36).

Iron is normally stored in ferritin, but in PD, ferritin levels are found to be inappropriately low. If the capacity of the neurons to store iron is exceeded, potentially toxic free iron will accumulate. As a severing factor neuro-melanin, which normally binds free iron, is released from dying neurons in the extracellular environment. This on the one hand, reduces the iron-binding capacity and on the other hand releases reactive iron and is able to activate microglia, increasing neuro-inflammation and leading to the neuronal death (36,40).

According to Zucca et al., potential reasons for the high accumulation of iron in the substantia nigra of PD patients and increasing vulnerability of dopaminergic neurons are:

i. increased permeability or dysfunction of blood-brain-barrier during the disease
ii. increased pro-inflammatory state, since neuro-inflammation can perturb iron homeostasis on different brain cells
iii. increased expression of lactoferrin receptors (involved in iron uptake through lactoferrin) in neurons and microvessels of the mesencephalon, with higher lactoferrin receptor immunoreactivity in substantia nigra of PD patients with higher dopaminergic nigral loss
iv. increased expression of a specific isoform of the divalent metal ion transporter 1 in the substantia nigra neurons of PD patients
v. decreased ferroxidase activity of ceruloplasmin, an iron-export ferroxidase essential for brain iron metabolism, in both the substantia nigra and cerebrospinal fluid form PD patients
vi. dysregulation of transferrin/transferrin receptor type 2 mediated iron transport in dopaminergic substantia nigra neurons of PD patients, particularly in their mitochondria
vii. mutations in genes coding for proteins involved in iron transport, binding, and metabolism

(List taken from Zucca F.A. et al. 2015, (37))

1.2.1 Iron Blood Parameters

There are controversial findings for the correlation of PD and iron blood parameters. A meta-analysis including a total of 520 PD subjects and 711 controls found no significant difference in serum-iron level (41).

Two case control studies including 50 PD patients each, found no statistically significant difference in serum iron and ferritin levels between PD patients and controls. In the study done by Mochizuki et al. symptoms' duration correlated inversely with serum iron and ferritin levels in contrast to the study done by Farhoudi et al., where no significant correlation was found between disease state and serum iron and ferritin levels (42,43).

A study based on mendelian randomisation (an approach based on the use of genes as instrumental variables, where genes known to modify iron levels were used as instruments to estimate the effect of iron on PD risk, based on estimates of the genetic effects on both serum-iron and PD) showed a protective effect of serum iron levels on PD, with a 3% relative reduction in PD risk per 10 mg/dl increase in iron (44).

Summarising increased concentrations of serum iron might be associated with a decreased risk of developing PD, thus showing a potentially protective effect of peripheral iron. On the other hand reduced concentrations of systemic iron are reported to be associated with an increased risk for PD, likely because of too low supplies of iron for synthesis of neurotransmitters, such as dopamine. Iron is an important cofactor of tyrosin hydroxilase, which is the key enzyme of dopamine synthesis. Moreover low iron concentrations are going along with low ferritin levels and reduced neuronal deposition of ferritin as it is found in substantia nigra of PD patients (45).

There is evidence that high iron concentrations and deposits in the brain increase the risk for PD and high peripheral iron concentration may even have protective effects. Taking all these results into consideration there seems to be a more complicated association between iron and PD, in which not total iron concentration of the body but its distribution is the key feature.

1.2.2 Iron in Cerebral Histology

There are several papers describing changes of iron content in post mortem histological analysis in basal ganglia of parkinsonian brains. The findings were reviewed in (34,38) and are summarised in Table 9. Different findings may be due to different stages of neurodegeneration as well as different dissection and tissue handling protocols. Furthermore sensitivities of used methods vary considerably (34).

Analysis	Substantia nigra	Putamen	Globus pallidus	Additional findings	Source
Semiquantiative					
Histological staining	normal		↑		Lhermitte et al. 1924 (46)
X-ray fluor. spectr.	General, but nonspecific increase in PD				Earle 1968 (47)
Energy disperse X-ray analysis	↑ (pars compacta, in neuromelanin				Jellinger et al. 1992 (48)

	granula)				
Quantitative					
Flame spectrophotometry	↑ (severely PD)	NSC	NSC	SN: ↑ferritin, ↑Fe^{3+}	Riederer et al. 1985 (49)
Inductively coupled plasma spectroscopy	↑ (total) ↑(pars compacta)	NSC (lateral) NSC (medial)	↓ (lateral) ↓ (medial)	↓ferritin (general and SN)	Dexter et al. 1989, 1990, 1991 (50-52)
	Significantly decreased ferritin levels in substantia nigra, caudate, putamen, globus pallidus, cerebral cortex, and cerebellum				
Laser microprobe mass analysis	↑ (in neuromelanin granula)				Good et al. 1992(53)
Extended X-ray absorption fine structure	↑	NSC	↑ (lateral)	↑ ferritin loading	Griffiths et al. 1999 (54)
Atomic absorption and atomic emission spectroscopy	NSC			also NSC frontal cortex, caudate nucleus, cerebellum	Utti et al. 1989 (55)
Colorimetry	NSC	NSC	↑	also NSC caudate, frontal cortex; transferrin NSC	Loeffler et al. 1995 (56)
Mössbauer spectroscopy	NSC				Galazka-Friedmann et al. 1996 (57)
Spectrophotometry	↑	NSC	NSC	also NSC cortex (Brodmann area 21), hippocampus	Sofic et al. 1988 (58)
Spectrophotometry	↑ Fe^{3+} (pars compacta),				Sofic et al. 1991 (59)
X-ray microprobe analysis	↑ (on zones lacking neuromelanin)			NSC central gray substance	Hirsch et al. 1991 (60)

Table 9. Post mortem histological analysis of changes in iron levels in basal ganglia in PD
↑↓: Significant change in iron mean values in PD compared with controls ($p<0,05$)
NSC: No statistically significant change
Table modified from (34,38)

1.2.3 Iron in Cerebral Imaging

There have been several attempts to visualise cerebral iron deposits in vivo and describe their correlation to PD. Most commonly used are Magnetic Resonance Imaging (MRI)-techniques and transcranial sonography (TCS) (39,61).

1.2.3.1 MRI Techniques

1.2.3.1.1 General MRI Techniques

Magnetic resonance imaging is an imaging technique, which uses an external magnetic field and radio frequency signals to produce image contrast: The patient is positioned in a strong external magnetic field, which induces magnetisation in his or her tissue. The magnetisation depends on the presence of magnetic nuclei, in the human body mainly hydrogen-ions (^{1}H protons), occurring mainly in water. Magnetic nuclei align roughly 50% parallel and 50% anti-parallel to the external field. However, this equilibrium would not allow signal generation, but at a closer look, there is a minimal overhead of 6 per 1 million protons aligning in a certain direction. This is called equilibrium magnetisation, which is equal to the longitudinal magnetisation. In addition to this, the spinning protons precess, which describes the fact that the rotation axis of a spin rotates for itself (like the wobbling of a child's spinning top). The hydrogen precession-frequency is called Lamor-frequency and is specific for each type of magnetic nucleus (e.g. 42MHz/T for ^{1}H). When radio frequency pulses at the specific Lamor-frequency are applied to the tissue, they cause a resonance phenomenon and flip the spinning protons to the transverse plane. The state, when the protons are spinning in the transverse plane, is called transverse magnetisation. This is an excited condition, so after the radio frequency signals have stopped, the protons diphase and the transverse magnetisation decays while the longitudinal magnetisation re-grows (those two phenomena are entitled as relaxation). During this period, the spinning protons send out characteristic radio frequency signals, which are measured and processed to MR images (62).

1.2.3.1.1.1 Magnetic Relaxation Times — T1 and T2 Images

The time required for the magnetisation to relax varies from one type of tissue to another, depending on multiple physical and chemical characteristics. Therefore, the individual relaxation times can be used to produce image contrast.

The principle of MRI techniques is measuring magnetisation rates represented by radio frequency signals sent out by dephasing protons in certain voxels at a specific time. The proton-dephasing is caused by two major effects: The first effect is based on interaction between the protons and their immediate molecular

environment with its naturally occurring molecular motion and causes re-growth of longitudinal magnetisation. The relaxation rate is called R1 and is the reciprocal of T1 relaxation time (R1=1/T1).

The other effect is the exchange of energy among the spinning nuclei in the transverse plane (spin-spin interactions), which results in a loss of transverse magnetisation. The relaxation rate is called R2 and is the reciprocal of T2 relaxation time (R2=1/T2).

The T1 value is the time required for the longitudinal-magnetisation to reach 63% of its maximum and the T2 value is the time required for 63% of the initial transverse magnetisation to decay. (62).

1.2.3.1.2 Magnitude Based Techniques for Quantification of Cerebral Iron Deposits

1.2.3.1.2.1 T2 (=1/R2)

The effect on relaxation times not only depends on the magnetic properties of a material, but also on the chemical environment. Small magnetic ions in solution, like free iron have their major effect by direct contact with water molecules (inner sphere mechanism) and reduce T1 to produce bright (hyperintense) signals on T1 –weighted images. Aggregates of magnetic particles largely shielded from the water by a protein shell, like ferritin and hemosiderin, the main source of iron content in the human brain, exert their effect on MR contrast by dephasing the magnetic spins of the protons diffusing in their vicinity (outer sphere mechanism). It reduces the T2 relaxation time of the protons and produces dark (hypointense) regions on T2 -weighted MR images. As ferritin and hemosiderin act through the outer sphere mechanism, the major effect of brain iron on MR images is a reduction (hypointensity) in T2, T2* and T2' and an enhancement of R2, R2* and R2' (hyperintensity) which are proportional to the concentration of paramagnetic iron ions (63,64).

However, there are also other factors influencing R2 values, like water concentration, which might adulterate iron values. These effects depend on the magnetic field strength and therefore another approach for calculating iron content is the field-dependent R2 increase (FDRI). Yet another approach is applying an additional radio frequency irradiation which enhances sensitivity of MRI to

molecular motion in the local susceptibility gradients, referred to as rotating frame longitudinal and transverse relaxations T1ρ and T2ρ (39,61,64-67).

1.2.3.1.2.2 T2* (=1/R2*)

Another effect, which produces relatively rapid dephasing of the nuclei and loss of transverse magnetisation, are inhomogeneities of the magnetic field within each individual voxel. This effect tends to mask the intrinsic T2 relaxation characteristics of the tissue. In other words, the actual transverse magnetisation relaxes much faster than the tissue characteristics would indicate. This real relaxation time is called T2* and is usually much less than T2. Again the reciprocal of the T2* relaxation time is the R2* relaxation rate. Several factors can contribute to field inhomogeneities and to T2* decay. One is the general homogeneity of the magnetic field. Another factor is that different tissues or materials in the body might have different magnetic susceptibilities. Susceptibility is a characteristic of a material that determines its ability to become magnetized when it is in an external magnetic field. If a region of tissue contains materials with different susceptibilities (e.g. iron), this results in a reduction of field homogeneity (62).

R2* is usually measured from gradient-echo sequences where the T2* effects are preserved. It combines T2 and T2' (see below) effects, which makes is a well-suited tool to measure iron content, but also more affected by local background sources of magnetic field variation and tissue specific characteristics other than iron that cause signal loss unrelated to the internal iron content of the tissue (39,61,64,65).

1.2.3.1.2.3 T2' (=1/R2')

The difference between R2* and R2 is R2' (1/T2'=R2' and R2*=R2+R2') (62).

R2' reflects reversible signal losses associated with local field inhomogeneity for instance due to the difference in relaxation rates because of susceptibility differences and is discussed to be more sensitive to iron content than R2. However, since R2' is very sensitive for signal changes it is vulnerable for perturbation.

Considering the pros and cons described above there is no ideal method for measuring tissue iron using MRI. One has to trade sensitivity for visualising iron specific effects against vulnerability to alterations (39,61,64,65).

1.2.3.1.3 Phase Based Techniques for Quantification of Cerebral Iron Deposits

The basic principle of phase-based techniques is the usage of phase information, often in combination with magnitude images. The phase describes the orientation of the magnetic moments of the protons in the transverse plane. After the application of a 90° flipping pulse, the nuclei are in the transversal plane and are rotating together in-phase. The precession rate, or resonant frequency, depends on the strength of the magnetic field where the nuclei are located. Nuclei located in field areas with different strengths spin (precess) at different rates. Here again iron is one cause for field inhomogeneities as described above (susceptibility effects). Others are background local fields that confound the effects of local phase changes in tissue or the chemical shift. The later refers to the affection of the resonant frequency of magnetic nuclei, such as protons, by the structure of the molecule in which they are located. The molecule structure shields the magnetic nuclei depending on its chemical structure, which means that protons in different chemical compounds will be in slightly different field strengths and will therefore resonate at different frequencies. As a result of these effects, some nuclei spin faster than others, which is boosted in the presence of iron. After a short period of time, the direction of the sum magnetisation begins to dephase. When measured, the phase information of the protons indicates the iron content among other minor tissue contributors (62,68).

1.2.3.1.3.1 SWI – Susceptibility Weighted Imaging

SWI uses differences in magnetic susceptibility to produce image contrast. As described above different susceptibilities cause field inhomogeneities and lead to proton dephasing. Phase imaging at sufficient long echo times (TE) in gradient echo sequences, provides excellent contrast between iron-laden tissues, gray matter, white matter, deoxygenated venous blood vessels, and other tissues with susceptibilities that are different from the background tissue (68,69).

Dephasing influences the frequencies of the radio frequent signals send out by the relaxing protons and measured by MRI. Therefore MRI-scans provide phase information (based on frequency changes) in addition to magnitude information (based on amplitude changes). The spin orientation of the protons and hence the

phase information can be imagined as arrows moving like the hand of a clock, which rotates in a circle measured in radian. Considering phase information, the position at a certain time is measured. This comes along with the problem that when for example the hand stands at 180° one cannot say if it rotated half a round (π) or one and a half rounds (3 π). This leads to image alterations ("phase wraps") and therefore the phase has to be unwrapped during post processing to overcome this problem.

SWI focuses on susceptibility effects and phase information as a tool to alter the contrast in magnitude images. However not only iron, but also other effects like air/tissue interfaces produce very high phase contrast. Another problem is the presence of background local fields that confound the effects of local phase changes in tissue. So there are several steps to create a susceptibility weighted image and measure tissue iron content: First the phase images are unwrapped and then high pass filtered to remove background field effects as good as possible. Second the filtered data is transformed by a special weighting mask and finally is multiplied by the magnitude image to create enhanced contrast between tissues with different susceptibilities (see Figure 3) (68,69).

Regional phase measurements are reported to significantly correlate with changes in regional brain iron concentration in gray matter structures (64,70). The benefit of SWI is that combining phase and magnitude information ensures the detectability of signal-intensity changes coming from both T2 and susceptibility differences between tissues. Measuring the two sources of information separately and combining the information during post-processing increases sensitivity for detecting iron, because this method takes full advantage of T2* signal-intensity losses in the magnitude image and susceptibility effects in the phase images to highlight both types of contrast in a single image (71).

1.2.3.1.3.2 QSM – Quantitative Susceptibility Mapping

Although clinically relevant, the big disadvantage of SWI is that it does not provide quantitative measures of magnetic susceptibility. The purpose of quantitative susceptibility mapping (QSM) is to overcome this limitation. While SWI generates contrast based on phase images, QSM further computes the underlying susceptibility of each voxel as a scalar quantity. Using phase information to produce contrast is problematic because MR phase is nonlocal and orientation-

dependent, thus not easily reproducible. Furthermore, it is difficult and not always reliable to differentiate diamagnetic susceptibility from paramagnetic susceptibility based on phase which means separating calcification which is diamagnetic from iron deposition which is paramagnetic is often not possible in SWI. Therefore, it is of great interest to determine the intrinsic property of the tissue, i.e., the magnetic susceptibility, from the measured signal phase (72). Moreover phase contrast does not exclusively reflect the local magnetic property of a voxel but is influenced by the magnetic properties of the surrounding tissue. For example, the phase and T2* contrast of a voxel with weak susceptibility may be due to susceptibility effects within the voxel or primarily come from nearby air-tissue interfaces which cast a cloud over the voxel of interest (73).

QSM is designed to calculate the intrinsic susceptibility for each voxel. To reach this target certain mathematical operations need to be done and certain problems need to be solved. Basically the magnetisation of each voxel is considered to be a magnetic dipole with an individual magnetic field which can be measured in MRI. The main problem is that the field to susceptibility inversion is ill-posed. Simplifying the term (in k-space/Fourier-domain, the virtual space where the MRI-data is collected and processed) which describes the connection between measured field parameters and susceptibility values can be describe as follows: Experimental measurement (phase) = Coefficient * Susceptibility distribution. To invert the point-wise multiplication a point-wise division would be the simplest approach. However the coefficient describes the dipole response to an external magnetic field in the k-space and contains among others k-space vectors. Now the problem is that the divisor under certain circumstances becomes zero, which is impossible. This results in two so-called zero cones in k-space, which are two conic surfaces at the so-called magic angle (54.7° from the main magnetic field) where susceptibility cannot be calculated. As a result there are large errors and many possible susceptibilities which present as streaking artefacts in the reconstructed susceptibility map. Therefore, the magnetic field-to-susceptibility inverse problem is ill-posed and lacks a unique solution. Another problem are again background fields or in other words the lack of MRI signal in regions with susceptibility sources outside the tissue of interest. Taking this into consideration two core elements of QSM are filtering background fields and solving the inverse problem. The general algorithm in QSM can be described as follows: Generate

magnitude image and phase information with unwrapping. → Remove background fields and generate tissue phase information. → Generate QSM from tissue phase and magnitude image. (Solving the inverse problem) → Quantitative susceptibility map (see Figure 3) (72-75).

There have been several attempts for solving the inverse field to susceptibility problem. For example Multiple Orientation Sampling (COSMOS), where an object is scanned and then rotated and scanned again which also leads to a rotation of the zero-cones in k-space. However this method requires multiple scans, which is not realizable in clinical practice (74). Therefore methods have been developed using mathematical models based on the information provided by a single orientated (mostly three-dimensional multi echo) gradient echo scan (73,75).

As described above QSM gives direct quantitative information on susceptibility in tissue und therefore is a very sensitive tool for measuring brain iron content. Langkammer et al. performed a post mortem validation study and compared iron values of different brain regions directly biochemically measured and information provided by QSM in the same subjects. They found strong linear correlation and confirmed that the magnetic susceptibility is very sensitive to variations in iron concentration in the human brain (76).

Murakami et al. compared QSM and R2* concerning estimating brain iron content in PD. The sensitivity, specificity, and accuracy of quantitative susceptibility mapping were considerably higher than the same values of R2* (77). Barbosa et al. and Du et al. performed similar studies and draw the same conclusion (78,79). Taking this into consideration QSM seems to be a superior method for in vivo measuring brain iron deposits.

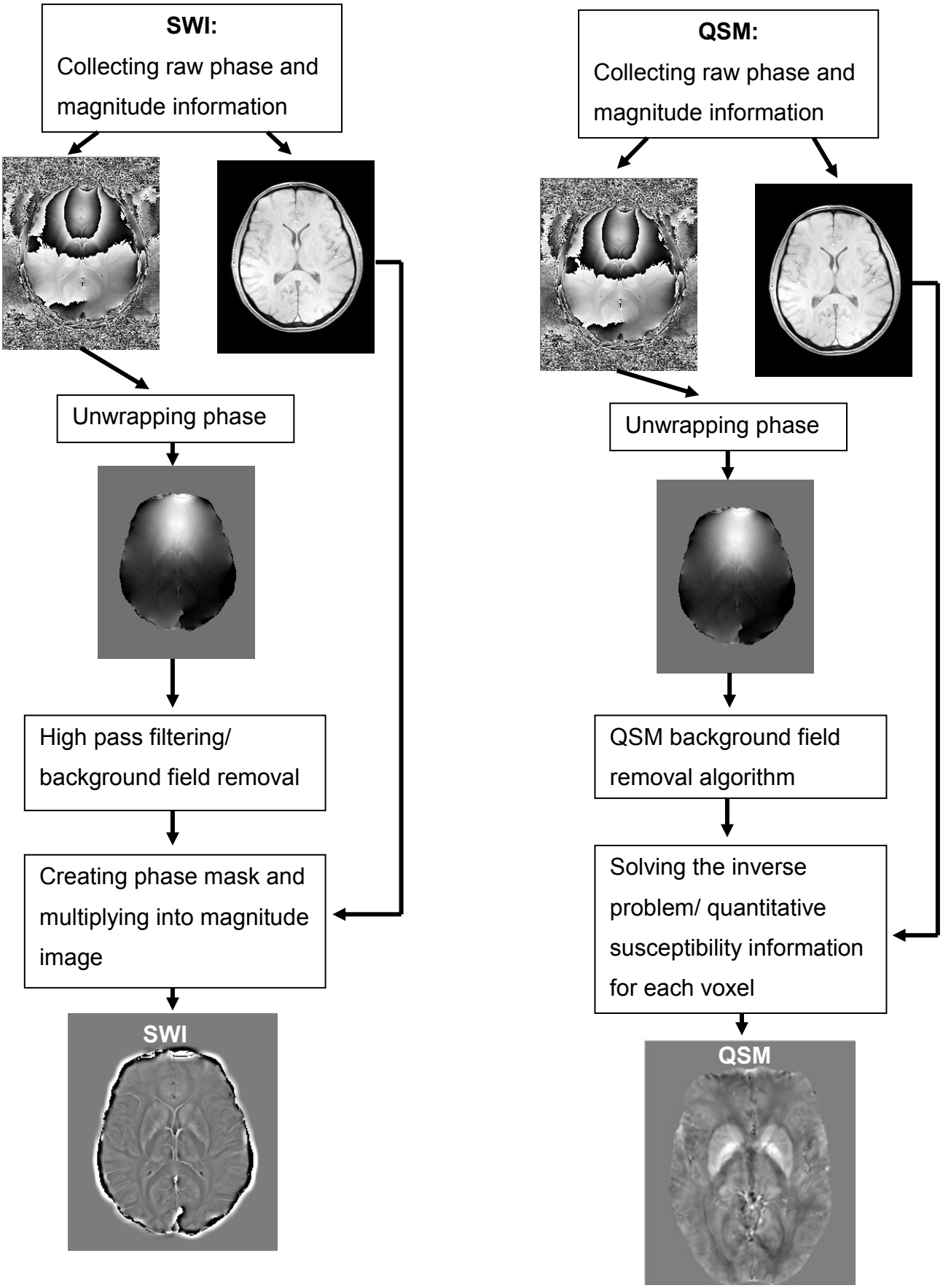

Figure 3. Schematic process of SWI and QSM

1.2.3.2 MRI – Cross-sectional

A PubMed search on “Parkinson AND iron AND MRI” gave 127 results. Studies on differences in iron levels in the basal ganglia between PD patients and normal controls are summarised in Table 10. In addition some groups also considered clinical symptoms, disease duration, age at onset, motor phenotype or differential diagnosis.

The findings vary and this may be due to different imaging techniques (sensitivity, image solution, slice thickness, region of interest (ROI) identification etc.) or differences in patients’ disease progression. Considering the results in Table 10 there seems to be a trend for significant higher iron deposits in the substantia nigra, especially pars compacta, in relation to healthy controls. The results on all other regions and clinical correlations are incoherent. This is in line with the histopathological findings summarised in Table 9.

MRI technique (Tesla) Patients/Controls	Substantia nigra	Putamen	Globus pallidus	Red nucleus	Additional findings	Source
T2 (1.5T) 30/33	↑iron ↓T2 no correlation with disease duration or clinical severity	↑iron ↓T2			Caudate: ↑iron ↓T2	Antonini et al. 1993 (80)
T1,T2 (1.5T) 23/18	NSC	NSC	NSC	NSC	Caudate, thalamus: NSC	Vymazal et al. 1999 (81)
T2 (1.5T) 25/27	NSC	NSC	NSC	NSC	Temporal cortex, frontal white matter, head of caudate: NSC	Mondino et al. 2002 (82)
T2 (1.5T) 20/16	SNc: ↑iron ↓T2 positive correlation with UPDRS and rigidity score SNr: NSC	NSC	NSC		Dentate nucleus: ↑iron ↓T2 Caudate: NSC	Atasoy et al. 2004 (83)
T2 (1.5T) 40/40	SNc: ↑iron ↓T2 higher p-value for more affected side, positive correlation with disease duration SNr: NSC	↓iron ↑T2	GPe: ↓iron ↑T2 inverse correlation with disease duration GPi: NSC		Caudate, subthalamic nucleus, locus ceruleus: NSC	Kosta et al. 2006 (84)

T2 (3T) 18/15	Patients who developed parkinsonism along with their existing dementia had significantly more iron in their substantia nigra than patients with Alzheimer disease alone.					Brar et al. 2009 (85)
R2' (1.5T) 12/13		↑iron ↑R2' pos. corr. with clinical symptoms UPDRSIII	↑iron ↑R2' pos. corr. with clinical symptoms		Thalamus: NSC	Ye et al. 1996 (86)
R2' (3T) 70/10	↑iron ↑R2' more affected side positively correlated to UPDRS III	↑iron ↑R2' rostral to caudal gradient, no clinical corr.				Wallis et al. 2008 (87)
T2' (1.5T) 30/24		↑iron	NSC		Caudate, thalamus: NSC T2' sign. different PSP from PD	Boelmans et al. 2012 (88)
R2, R2*, R2' (3T) 12/10	↑iron ↑R2* ↑R2' ↓R2					Gorell et al. 1995 (89)
R2,R2*,R2' (1.5T) 25/14	↑iron ↑R2* ↑R2'	↓iron ↓R2' pos. corr. with disease duration R2*: NSC	NSC		Caudate, frontal white matter: NSC UPDRS, age at onset: NSC	Graham et al. 2000 (90)
T2* (2T) 45/45	SNc: ↑iron ↓T2*	↓iron ↑T2* (PD>10 years)	↓iron ↑T2* (PD>10 years)			Ryvlin et al. 1995 (91)
T2*(3T) 20 (early PD)/ 20	↑iron ↓T2*					Baudexel et al. 2010 (92)
R2* (3T) 30/22	↑iron	NSC	NSC	NSC	Caudate, thalamus: NSC	Peran et al. 2010 (93)
R2*, diffusion tensor imaging 16/16	↑iron ↑R2* ↓fractional anisotropy UPDRS: NSC					Du et al. 2011 (94)
R2* (3T) 40/29	↑iron ↑R2* positively correlated to disease duration, L-dopa equivalent dose & UPDRS III				SN and GP iron negatively correlated to serum cholesterol	Du et al. 2012 (95)
R2* (3T) 20/20	NSC (SN, SNc, SNr)	NSC	NSC		Caudate, Thalamus, Nc. accumbens:	Bunzeck et.al. 2013 (96)

					NSC Putamen, caudate and thalamus R2* correlated positively with tremor dominant motor phenotype	
T2*/ESWAN (3T) 20/14	↑iron ↓mean phase value (SNc, SNr), also correlated to disease stage			NSC		Wang et al. 2013 (97)
R2* (3T) 38/23	↑iron ↑R2* positively correlated to disease duration & UPDRS III			↑iron ↑R2* positively correlated to UPDRS III & dyskinesia		Lewis et al. 2013 (98)
R2* (1.5T) 42/20	NSC					Aquino et al 2014 (99)
T2* (9.4T) Rat model	NSC				↑striatal iron accumulation	Virel et al. 2014 (100)
R2* (3T) 20/20	↑iron ↑R2* UPDRS: NSC (also symptomatic and asymptomatic LRRK2 or Parkin mutation carriers)	NSC	NSC	NSC	Caudate, thalamus: NSC	Pyatigorskaya et al. 2015 (101)
T2* (3T) 22 (early stage/de novo PD)/10	NSC (SN, SNc, SNr)					Reimao et al 2016 (102)
T2ρ (4T) 8/8	↑iron ↓T2ρ					Michaeli et al. 2007 (66)
T1ρ, T2ρ (4T) 9/10	↑iron ↑T1ρ ↓T2ρ				T1ρ asymmetry correlating to asymmetry in motor features (UPDRS)	Nestrasil et al. 2010 (67)
field-dependent R2 increase (FDRI) (1.5/0.5T) 12/14	early onset PD: ↑ferritin late onset PD: ↓ferritin	early onset PD: ↑ferritin	early onset PD: ↑ferritin		Decreased ferritin levels and increased free iron levels in the SN of later onset PD subjects suggesting dysregulation of iron metabolism occurs in PD and that it may differ in earlier- versus later-onset PD.	Bartzokis et al. 1999 Bartzokis et al. 2004 (103,104)
SWI (1.5T) 42/30	SNc: ↑iron ↓SWI positive correlation with	NSC	NSC	↑iron ↓SWI	Caudate, white matter, grey matter, liquor: NSC	Zhang et al. 2009 (105)

	UPDRS III, only more affected side SNr: NSC					
SWI (3T) 40/26	↑iron ↓SWI (only more affected side) positive correlation with UPDRS, NSC for disease duration and age at onset	NSC	NSC	NSC	Caudate, thalamus, frontal white matter: NSC	Zhang et al 2010 (106)
SWI (3T) 30/19	↑iron	NSC	↑iron	NCS	Caudate: NCS SWI sign. different Hoehn-Yahr III-IV from I-II	Huang et al. 2010 (107)
SM (7T) 9/11	SNc: ↑iron SN: NSC					Loitfipour et al. 2012 (108)
SWI (3T) 87/50	No significant correlation of SWI values and PD motor phenotype.					Jin et al 2012 (109)
SWI (1.5T) 16/44	↑iron	↑iron, split in 4 regions, sign. DD PD vs. MSA-P	↑iron	NSC	Caudate, thalamus: NSC	Wang et al. 2012 (110)
SWI, R2* (3T) 36/21	↑iron		↑iron			Rossi et al. 2013 (111)
SWI (3T) 54(early/ advanced stage PD)/40	↑iron ↓SWI	↑iron ↓SWI	↑iron ↓SWI	↑iron, ↓SWI ↑iron correlating with disease state	Head of caudate: ↑iron, iron positively correlating with disease state	Wu et al. 2014 (112)
QSM, R2, R2* (3T) 20/30	↑iron (SN, SNc) ↑QSM, ↑R2 ↑R2* only SNc	NSC	NSC	NSC	Caudate, thalamus: NSC	Barbosa et al 2015 (78)
QSM, R2* (3T) 47/47	SNc: ↑iron ↑QSM, ↑R2*				R2*: no correlation to clinic QSM: positive correlation to disease duration, UPDRS II, L-Dopa equivalent dose	Du et al. 2015 (79)
QSM, R2* (3T) 44 (early state)/35	↑iron ↑R2* ↑QSM positively correlated with disease duration & UPDRS III	↑iron ↑QSM R2*: NSC	NSC	↑iron ↑QSM, R2* NSC	Head of caudate: NSC	He et al. 2015 (113)
QSM, R2* (3T) 21/21	↑iron ↑ R2* ↑QSM	NSC	NSC	NSC	Head of caudate, thalamus: NSC	Murakami et al. 2015 (77)

Table 10. Overview about PubMed search for literature relating to differences in MRI iron levels in the basal ganglia between PD patients and healthy controls
↑↓: Significant change in iron/ MRI parameters in PD compared with controls (p<0,05)
NSC: No statistically significant change

1.2.3.3 MRI – Longitudinal

In contrast to cross-sectional studies, there are only very little data on longitudinal changes of iron in PD, which are summarised in Tables 11-13.

There was a trend for longitudinal increase in iron content in substantia nigra in PD patients with significant results in R2* in one (114) and for lateral substantia nigra pars compacta in T2 in another study (115). Results for other brain regions varied considerably.

Correlations to clinical parameters were incoherent: On the one hand, R2* change in substantia nigra pars compacta and substantia nigra pars reticulata positively correlated with UPDRS III change whereas no correlation to Hoehn and Yahr Scale or L-dopa equivalent dose was found (114). Lateral substantia nigra pars compacta R2* change positively correlated with UPDRS III change and PDQ-39 mobility subscore change and values tended to increase in patients with higher UPDRS III scores und decrease in those with lower scores. Moreover there was a greater change in patients, who showed freezing than in those who did not.(116). On the other hand, no significant correlation between MMSE, disease duration, UPDRS III, UPDRS III change or age and MRI parameters was found (115).

Ulla et al. found significant higher iron increase in the substantia nigra pars compacta and pars reticulate as well as in the caudal putamen in PD patients than in healthy controls (114), whereas other authors did not describe differences (115,116).

Ulla et al. 2013 R2* (1.5T) **Baseline:** 27 PD/ 26 controls **Follow-up 3 years:** 18 PD/ 14 controls					
Subject	**Substantia nigra**	**Putamen**	**Globus pallidus**	**Grey/ white matter**	**Additional findings**
Baseline	SNc, SNr: ↑iron ↑ R2*	NSC	NSC	NSC	Gender, disease duration, Hoehn and Yahr, UPDRS III: NSC
Longitudinal change PD	SNc: ↑10.2%, p=0,001 SNr: ↑8.1%,, p=0.042	caudal: ↑11.4%, p=0,011 rostral: NSC	NSC	Grey matter: NSC White matter:	R2* change in SNc (p=0.021) and SNr (p=0.021) positively correlates with UPDRS III change. No correlation to Hoehn and Yahr or L-dopa equivalent dose.

				↓7.5%, p=0.042	
Longitudinal change controls	No significant change in iron content.				
Longitudinal change PD vs. controls	SNc: p=0.002 SNr: p=0.033	caudal: p=0,022 rostral: NSC	NSC	NSC	

Table 11. Longitudinal changes in MRI iron levels in the basal ganglia of PD patients and healthy controls according to Ulla et al. 2013 (114)
↑↓: Significant change in iron/ MRI parameters (p<0,05)
NSC: No statistically significant change

Wieler et al. 2015 R2* (3T) **Baseline:** 19 early untreated PD/ 13 controls **Follow-up1 1.5 years, Follow-up2 3 years**					
Subject	**Substantia nigra compacta**	**Substantia nigra reticulata**	**Putamen**	**Globus pallidus**	**Additional findings**
Baseline	lateral SNc: ↑iron ↑ R2* medial SNc: NSC	NSC	NSC	NSC	
FU1 & FU2	No significant change in iron content in any region.				
Longitudinal change baseline to FU2 PD	R2* change in lateral SNc positively correlates with UPDRS III change (p=0.008) and PDQ-39 mobility subscore change (p=0.03). Greater change in patients, who showed freezing than in those who did not.				Lateral SNc R2* values tended to increase in these with higher UPDRS III scores und decrease in those with lower scores.

Table 12. Longitudinal changes in MRI iron levels in the basal ganglia of PD patients and healthy controls according to Wieler et al. 2015 (116,117)
↑↓: Significant change in iron/ MRI parameters (p<0,05)
NSC: No statistically significant change

Rossi et al. 2014 T2, T2*, SWI (3T) **Baseline:** 32 early PD/ 19 controls **Follow-up 2 years** 25 PD/ no controls					
Subject	**Substantia nigra compacta**	**Substantia nigra reticulata**	**Putamen**	**Globus pallidus**	**Additional findings**
Differences PD to controls	Variable findings for specific regions in different imaging techniques. No significant change in iron content in any region after correction for multiple comparisons.				
Longitudinal change baseline to follow-up PD	medial SNc: ↑iron ↓T2 R2*, SWI: NSC	NSC	NSC	anterior: ↑iron ↓T2 R2*, SWI: NSC	Red nucleus, nucleus dentatus, caudate, thalamus, basilar pons: NSC

	lateral SNc: NSC			posterior: NSC	
Clinical correlation	No significant correlation between MMSE, disease duration, UPDRS III, UPDRS III change or age and MRI parameters. In the globus pallidus anterior and medial SNc, the change was associated with mild cognitive impairment. In the caudate nucleus, the increase was pronounced in patients with disease onset at 67 years or older.				

Table 13. Longitudinal changes in MRI iron levels in the basal ganglia of PD patients and healthy controls according to Rossi et al. 2014 (115)
↑↓: Significant change in iron/ MRI parameters ($p<0,05$)
NSC: No statistically significant change

1.2.3.4 Iron in Transcranial Sonography

In TCS about 90% of PD patients show substantia nigra hyperechogenicity which may be due to increased iron deposits. Substantia nigra hyperechogenicity in healthy subjects is thought to go along with an increased risk for developing PD. Gröger et al. reviewed studies concerning this matter and drew the conclusion that increased iron levels contribute to this sonographic abnormality and possibly indicate iron accumulation as a very early process in the pathogenesis of PD (61).

2 Materials and Methods

2.1 Subjects

The study sample was drawn from the prospective, longitudinal registry on movement disorders in Graz (PROMOVE). The patients were recruited from the movement disorders outpatient clinic at the University Clinic for Neurology Graz, they were all fully informed and gave written consent. The local ethics committee of the Medical University of Graz gave its positive vote, number 21-345 ex 09/10.
Since January 2010 over 300 patients have been included. The study-design includes a baseline examination and four follow-ups including clinical testing, blood parameters and imaging techniques.

General Inclusion Criteria:

- Verified diagnosis of a movement disorder
- Age of 18 or older
- MMSE-score over 24 to be allowed to sign the consent form, otherwise there had to be a solicitor to sign the form

General Exclusion criteria:

- Age under 18
- No commitment from the patient or his or her solicitor to sign the consent form
- Patients who did not have a solicitor and the study-doctor declared the patient not to be able to sign the consent form himself or herself
- Patients who undergo a study for experimental medical treatment of their movement disorder

To be included in the current investigation the following criteria had to be fulfilled: Diagnosis of PD according to the UK Parkinson's Disease Society Brain Bank criteria (25), availability of a detailed neurological examination and of a comprehensive MRI examination at baseline and after a follow-up period of approximately 2 years (mean 2.05, SD 0.12, min 1,69, max 2.28). A total of 32 PD patients were included, for patients' characteristics see Table14.
As controls 15 age-matched patients (mean age 56.90 ± 15.31, t-test p-value 0.094, 6 male, 9 female) from the PROMOVE study cohort with a clinically verified

diagnosis of a non-degenerative tremor syndrome (essential tremor (n=7), dystonic tremor (n=8)) were selected.

	Mean ± SD	Minimum	Maximum
Age [years]	63.30 ± 10.03	30.89	75.71
Sex	Male: 23 (71.9%), Female: 9 (28.1%)		
Disease duration [years]	4.59 ± 4.81	0.26	20.98
Education [years]	11.06 ± 1.44	8	16

Table 14. Characteristics of PD patients at baseline examination

2.2 Clinical Assessment

Clinical examinations in the PD group were done under medication in a practical ON-state. Patients' clinical state at baseline and follow-up was assessed using the Hoehn & Yahr scale (20) and the Movement Disorder Society (MDS)-sponsored revision of the Unified Parkinson's Disease Rating Scale (MDS-UPDRS) (26). Sub scores for Part I (non-motor experiences of daily living), Part II (motor experiences of daily living), Part III (motor examination) and Part IV (motor complications) und total-UPDRS-scores were calculated. Patients were classified as tremor dominant (TD, n=24), postural instability/gait difficulty (PIGD, n=5) or indeterminate (n=3) on the basis of their MDS-UPDRS performance (118). For statistical analysis PIGD and indeterminate patients were merged and the group was divided in tremor-dominant (TD) and non-tremor-dominant (NTD) patients. To define the clinically more affected side the MDS-UPDRS III items at baseline examination for each side were summed and with a difference of two or more points patients were categorised as right-side-dominant (n=17) or left-side-dominant (n=15) (119). Additionally tremor was evaluated by the Fahn-Tolosa-Marin tremor rating scale (FTM) (120,121) and non-motor symptoms were enquired using the Nonmotor Symptoms Questionnaire (NMS) (122,123).

The L-dopa equivalent dose (LED) was calculated on the basis of prescribed medication at the assessment-time (124).

To evaluate cognition patients underwent a CERAD-Plus testing (125). The ''Consortium to Establish a Registry for Alzheimer's disease (CERAD) – Plus'' neuropsychological test battery includes test for verbal fluency, the modified Boston Naming Test, Mini Mental Status Examination (MMSE), a word list memory test, constructional praxis, word list recall and word list recognition. The CERAD-

Plus is enhanced by the Trail Making Test (TMT) parts A and B as well as phonematic fluency (s-words). Moreover CERAD total scores (including verbal fluency, modified Boston Naming Test, constructional praxis, word list memory, word list recall and word list discriminability for TS1 and additionally constructional recall for TS2) (126,127) and a memory score (including word list recall, word list recognition and constructional recall) (128) were calculated.

2.3 MRI

2.3.1 Data Acquisition

All patients in the PD and control group underwent two 3 Tesla cerebral-MRI-scans (TimTrio, Siemens Healthcare, Erlangen, Germany) using a head coil array with 12 receiver channels.

2.3.2 Image Processing and Analysis

R2* was reconstructed from gradient echo sequences, acquired with the identical spoiled 3D FLASH sequence, with 6 equally spaced echoes (TR/TE1/FA, 35 ms/4.92 ms/20°; inter-echo spacing, 4.92 ms; in-plane resolution, 0.9x0.9 mm²; slice thickness, 2 mm; number of slices, 64; acquisition time, 4 minutes 51 seconds).

For R2* gradient echo images were registered to the first echo to correct for image shifts induced by the bipolar readout gradient and R2* was then calculated voxel-wise by applying a noise truncation model and mono-exponential fitting (129).

The automated segmentation of regions of interest was done on an anatomical T1-weighted 3D MPRAGE sequence with 1 mm isotropic resolution (TR/TE/TI/FA, 1900 ms/2.19 ms/900 ms/9°; acquisition time, 6 minutes 1 second). The bilateral caudate nucleus, globus pallidus, putamen and thalamus were segmented using FreeSurfer (130).

Substantia nigra and its sub-regions pars compacta and pars reticulata have very poor contrast on conventional MR-images, which makes automatic segmentation vulnerable for mistakes. To overcome this problem a largely iron-independent form of contrast was developed, which combines MTR (magnetisation transfer imaging) and R2 images:

1. Registration of noMTC (MTR scan without MT pulse) on R2 scan (pdT2) and creating of a registration-matrix.

2. Registration of MTR image (calculated from noMTC and MTC scans) using the registration-matrix from above.
3. Normalising of S0 (calculated from the 2 echoes from turbo-spin echo sequence "pdT2", S0 is the zero-crossing on the y-axis of the filtered mono-exponential curve of the two echoes). As maximum an empirical factor of 1900 was used in all scans.
4. Inverting of S0 (1-S0_normalised)
5. The contrast is the mean from S0_inverted and MTR ((1 - S0/1900) + MTR)/2

On these images substantia nigra as well as the sub-regions were drawn manually by one rater for both groups. Figure 4 shows an example for segmentation of substantia nigra.

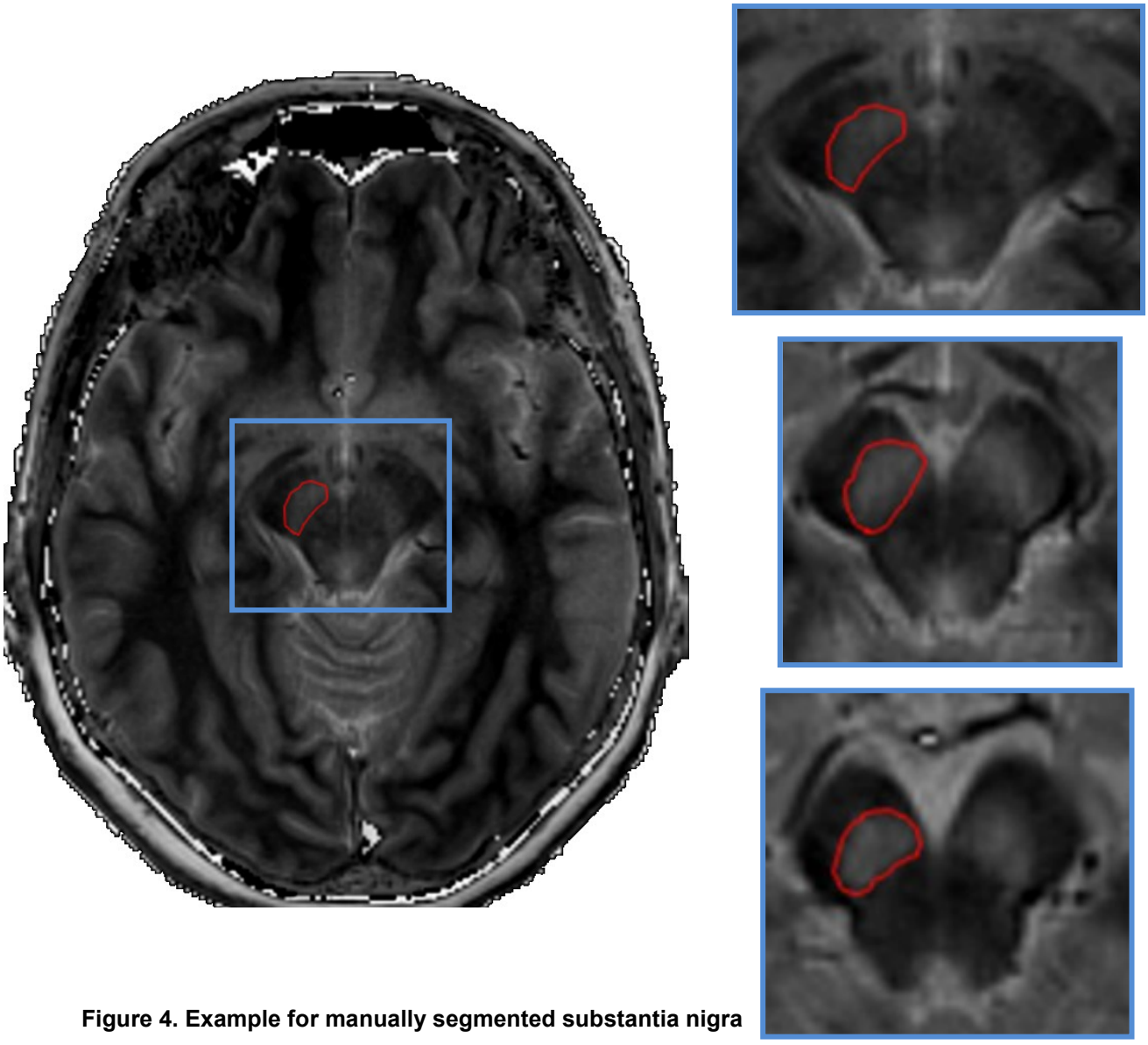

Figure 4. Example for manually segmented substantia nigra

2.4 Statistical Analysis

All statistical analyses were performed using the software SPSS Statistics (IBM Statistics for Windows, Version 23, Armonk, NY, USA). A p–value of $p < 0.05$ was considered as statistically significant. Assumptions of normal distribution were tested with the Kolmogorov–Smirnov test. Normally distributed variables are shown as mean ± standard-deviation (SD) and non-normally distributed variables as median and interquartile range. For longitudinal data analysis, repeated measure ANOVAs with time as inner-subject-factor were done: In the PD group global R2* values as well as R2* values only contralateral to the clinically more affected side for each ROI and clinical parameters were tested with correction for disease duration. The same analysis was repeated with correction for age, sex and disease duration and for R2* values with TD and NDT as between-subject-variable. Significant results were corrected with Bonferroni correction for multiple comparisons. For significant results in the ANOVAs Pearson's correlation analyses with correction for disease duration were performed.

To compare R2* in PD and control group repeated measure ANOVAs for each ROI with time as inner-subject-factor and group as between-subjects factor were performed. Additionally t-tests for independent samples for R2* values at baseline and follow-up as well as for differences were done.

3 Results

3.1 Longitudinal MRI Analysis of Iron Content and Clinical Development in PD

Table 15 shows mean R2* values and clinical parameters at baseline and follow-up examination in the PD-group (n=32). The development over the 2 year follow-up period is shown as mean difference (follow-up minus baseline) and significance of repeated measure ANOVAs on the one hand corrected for disease duration alone, on the other hand corrected for disease duration, age and sex.

R2* values tended to increase in all ROIs except in the thalamus, where there was no change. A significant increase was found in the substantia nigra and its sub regions pars compacta and pars reticulata. When correcting for multiple comparisons only total substantia nigra values remained significant. R2* development corrected for age, sex and disease duration showed no significant result in any region.

For clinical parameters only L-dopa equivalent dose increased significantly. Hoehn and Yahr scale showed significant increase, when correcting for disease duration alone and MDS-UPDRS IV as well as Nonmotor Symptoms Questionnaire when correcting for age, sex and disease duration. These results did not remain significant after correction for multiple comparisons. There was a trend for improvement in MDS-UPDRS III, FTM tremor rating scale and all cognitive parameters.

Parameter	Baseline (mean ± SD)	Follow-Up (mean ± SD)	Mean Difference	95% Confidence Interval for Difference		Significance[a]	Significance[b]
				Lower Bound	Upper Bound		
R2* Caudate Nucleus	23.40±2.26	23.52±2.08	0.124	-0.543	0.791	0.305	0.232
R2* Pallidum	38.85±5.52	40.68±5.89	1.835	0.336	3.333	0.081	0.992
R2* Putamen	27.91±3.67	28.42±3.26	0.509	-0.088	1.106	0.171	0.665
R2* Thalamus	20.86±1.11	20.85±1.21	-0.007	-0.365	0.350	0.351	0.629
R2* Substantia nigra	34.15±4.96	35.87±5.26	1,714	0.214	3.213	**0.005 (0.025)**	0.691
R2* Substantia	29.89±3.53	31.42±4.62	1.517	-0.122	3.156	**0.011** (0.068)	0.660

Nigra Pars Compacta							
R2* Substantia Nigra Pars Reticulata	38.12±6.93	39.77±6.68	1.650	-0.194	3.494	**0.049** (0.076)	0.837
LED	220.75±219.59	518.88±303.45	298.125	220.239	376.011	**0.000 (0.000)**	**0.000 (0.000)**
MDS-UPDRS I	6.22±4.01	7.13±5.69	0.906	-0.861	2.674	0.242	0.122
MDS-UPDRS II	9.78±4.56	11.41±6.22	1.625	-0.040	3.290	0.144	0.922
MDS-UPDRS III	28.22±11.95	27.81±11.67	-0.406	-4.4461	3.649	0.779	0.153
MDS-UPDRS IV	0±0	0.16±0.723	0.156	-0.066	0.397	0.193	**0.001** (0.162)
MDS-UPDRS total	44.22±16.30	46.50±19.35	2.281	-3.785	8.347	0.323	0.212
Hoehn & Yahr	1.91±0.39	2.06±0.35	0.156	-0.010	0.323	**0.045** (0.058)	0.286
NMS	7.25±4.37	7.66±4.71	0.406	-0.832	1.645	0.846	**0.038** (0.507)
FTM	11.09±9.61	7.94±10.16	-3.156	-5.583	-0.730	0.294	0.225
CERAD TS1	78.78±9.10	79.69±13.28	0.906	-2.374	4.187	0.239	0.855
CERAD TS2	88.38±10.11	89.25±14.71	0.875	-2.528	4.278	0.353	0.840
CERAD MS	35.13±3.97	35.97±4.55	0.844	-0.612	2,300	0.567	0.857
MMSE	27.84±1.63	28.28±1.65	0.438	-0.115	0.990	0.562	0.096
TMT a	54.87±29.39	53.53±39.12	-1.344	-12.166	9.479	0.733	0.718
TMT b	132.94±85.30	124.34±79.69	-8.594	-32.120	14.932	0.560	0.893

Table 15. Descriptive statistics and repeated measure ANOVA of longitudinal change of global R2* values and clinical parameter in the PD group.
[a]Repeated Measure ANOVA, corrected for disease duration, if significant in parentheses significance of mean difference with Bonferroni correction for multiple comparisons
[b]Repeated Measure ANOVA, corrected for, age, sex and disease duration, if significant in parentheses significance of mean difference with Bonferroni correction for multiple comparisons

Table 16 lists R2* values and their development only contralateral to the clinically more affected side. Total substantia nigra and pars compacta, corrected for disease duration, showed significant increase without correction for multiple comparisons. Other than that, there were no significant results.

Parameter	Baseline (mean ± SD)	Follow-Up (mean ± SD)	Mean Difference	95% Confidence Interval for Difference		Significance[a]	Significance[b]
				Lower Bound	Upper Bound		
R2* values contralateral to the clinically more affected side							
R2* Caudate Nucleus	23.58±2.42	23.80±2.46	0.221	-0.684	1.126	0.108	0.284
R2* Pallidum	38.63±6.00	40.30±5.79	1.675	0.052	3.298	0.192	0.138
R2* Putamen	27.79±3.68	28.05±3.61	0.264	-0.583	1.110	0.673	0.939
R2* Thalamus	20.83±1.50	20.90±1.34	0.070	-0.451	0.592	0.969	0.767
R2* Substantia nigra	34.38±5.63	36.04±5.86	1.662	-0.286	3.610	**0.043** (0.087)	0.786

R2* Substantia Nigra Pars Compacta	30.19±4.10	31.91±5.61	1.717	-0.346	3.780	**0.017** (0.100)	0.776
R2* Substantia Nigra Pars Reticulata	38.69±8.33	40.31±8.24	1.623	-1.267	4.513	0.356	0.917

Table 16. Descriptive statistics and repeated measure ANOVA of longitudinal change of R2* values contralateral to the clinically more affected side in the PD group.
[a]Repeated Measure ANOVA, corrected for disease duration, if significant in parentheses significance of mean difference with Bonferroni correction for multiple comparisons
[b]Repeated Measure ANOVA, corrected for, age, sex and disease duration, if significant in parentheses significance of mean difference with Bonferroni correction for multiple comparisons

Table 17 illustrates R2* values and their longitudinal development in tremor-dominant (TD, n=24) and non-tremor-dominant (NTD, n=8) PD patients. There was no significant difference in any region for total R2* values as well as for R2* values only contralateral to the clinically more affected side. In the thalamus, total R2* values tended to decrease in the TD group and increase in the NTD group, however the significance got lost after correction for multiple comparisons.

Parameter	Type[a]	Baseline (mean ± SD)	Follow-Up (mean ± SD)	Significance[b]	Mean Difference NTD-TD	Significance[c]
R2* Caudate Nucleus	TD	23.28±2.22	23.75±2.49	0.545	0.100	0.434
	NTD	23.57±2.17	23.39±1.90			
R2* Pallidum	TD	39.04±5.24	40.57±5.54	0.065	-0.158	0.489
	NTD	38.29±6.64	41.01±7.22			
R2* Putamen	TD	27.87±3.82	28.38±3.54	0.214	0.111	0.972
	NTD	28.01±3.42	28.53±2.45			
R2* Thalamus	TD	20.82±1.07	20.56±1.15	**0.041**	0.680	**0.008** (0.114)
	NTD	21.00±1.30	21.76±0.92			
R2* Substantia nigra	TD	33.69±4.71	35.27±5.38	0.007	2.110	0.681
	NTD	35.54±5.77	37.64±4.74			
R2* Substantia Nigra Pars Compacta	TD	29.69±3.60	30.84±4.93	0.008	1.580	0.374
	NTD	30.47±3.48	33.08±3.18			
R2* Substantia Nigra Pars Reticulata	TD	37.42±6.60	39.31±6.59	0.104	2.276	0.700
	NTD	38.12±6.93	41.17±7.15			
	R2* values contralateral to the clinically more affected side					
R2* Caudate Nucleus	TD	23.50±2.43	23.71±2.77	0.137	0.750	0.913
	NTD	23.82±2.54	23.80±2.46			
R2* Pallidum	TD	38.75±5.52	40.24±5.33	0.188	-0.124	0.721
	NTD	38.27±7.62	40.31±5.79			
R2* Putamen	TD	27.67±3.78	28.04±3.64	0.846	0.233	0.657
	NTD	28.16±3.57	28.08±3.77			
R2* Thalamus	TD	20.72±1.55	20.60±1.30	0.575	0.428	0.211
	NTD	21.18±1.37	21.81±1.04			
R2* Substantia nigra	TD	34.15±5.58	35.51±5.81	0.039	1.484	0.538
	NTD	35.04±6.12	31.62±6.09			
R2*	TD	30.29±4.25	31.44±5.83	0.010	0.791	0.284

Substantia Nigra Pars Compacta	NTD	29.89±3.87	33.32±4.96			
R2* Substantia Nigra Pars Reticulata	TD	37.90±7.94	39.62±8.12	0.436	2.916	0.906
	NTD	41.08±9.53	42.40±8.82			

Table 17. Descriptive statistics and repeated measure ANOVA of longitudinal change of R2* values, comparison of tremor-dominant to non-tremor-dominant subjects
[a]Clinical dominance type. TD: tremor-dominant (n=24), NTD not tremor-dominant (n=8)
[b]Repeated Measure ANOVA, corrected for disease duration, general significance
[c]Repeated Measure ANOVA, corrected for disease duration, significance for difference between types. If significant in parentheses significance of mean difference with Bonferroni correction for multiple comparisons

3.2 Correlation with Clinical Data

Table 18 shows Pearson's correlation analyses with correction for disease duration of differences in R2* values and clinical parameters, which showed significant effects in the ANOVAs. There was a slightly significant negative correlation between difference in LED and difference in R2* in global substantia nigra pars reticulata as well as between Hoehn and Yahr scale and R2* in total substantia nigra contralateral to the clinically more affected side.

Partial correlation, corrected for disease duration: correlation (significance)			
	∆ LED	∆ Hoehn & Yahr	∆ NMS
∆ R2* Substantia nigra	-0.240 (0.193)	0.131 (0.482)	-0.098 (0.601)
∆ R2* Substantia Nigra Pars Compacta	-0.318 (0.081)	0.020 (0.917)	-0.159 8 (0.393)
∆ R2* Substantia Nigra Pars Reticulata	**-0.357 (0.049)**	0.170 (0.360)	-0.322 (0.078)
R2* values contralateral to the clinically more affected side			
∆ R2* Substantia nigra	-0.126 (0.500)	**-0.356 (0.049)**	-0.280 (0.128)
∆ R2* Substantia Nigra Pars Compacta	-0,276 (0.133)	-0.333 (0.067)	-0.337 (0.064)
∆ R2* Substantia Nigra Pars Reticulata	-0.014 (0.579)	-0.262 (0.155)	-0.352 (0.052)

Table 18. Pearson's correlation analyses with correction for disease duration of differences in R2* values and clinical parameters, which showed significant effects in the ANOVAs

3.3 Comparison with Controls

3.3.1 Longitudinal Development

Table 19 shows R2* values and their longitudinal development as repeated measure ANOVAs of PD and control subjects. Table 20 lists mean differences over time in R2* values in both groups, compared by a t-test. There was no significant difference between R2* change in PD and control group. However there

was a trend for higher R2* increase in the PD group in all regions, especially in substantia nigra.

Parameter	Groupe[a]	Baseline (mean ± SD)	Follow-Up (mean ± SD)	Significance[b]	Mean Difference PD-CONT	Significance[c]
R2* Caudate Nucleus	PD	23.40±2.26	23.52±2.08	0.930	-0.392	0.572
	CONT	23.94±2.32	23.77±2.49			
R2* Pallidum	PD	38.85±5.52	40.68±5.89	0.028	0.439	0.525
	CONT	38.81±5.26	39.84±5.55			
R2* Putamen	PD	27.91±3.67	28.42±3.26	0.276	0.302	0.497
	CONT	27.90±3.73	27.92±3.05			
R2* Thalamus	PD	20.86±1.11	20.85±1.21	0.142	0.192	0.153
	CONT	20.93±1.39	20.41±1.42			
R2* Substantia nigra	PD	34.15±4.96	35.87±5.26	0.169	5.686	0.218
	CONT	29.27±2.90	29.37±3.86			
R2* Substantia Nigra Pars Compacta	PD	29.89±3.53	31.42±4.62	0.117	5.000	0.511
	CONT	25.30±2.67	25.99±3.96			
R2* Substantia Nigra Pars Reticulata	PD	38.12±6.93	39.77±6.68	0.198	6.303	0.518
	CONT	32.37±4.49	32.92±4.30			

Table 19. Descriptive statistics and repeated measure ANOVA of longitudinal change of R2* values, comparison of PD and control subjects
[a]PD: Parkinson's disease (n=32), CONT: Control group (n=15)
[b]Repeated Measure ANOVA, general significance
[c]Repeated Measure ANOVA, significance for difference between groups.

Parameter	PD (mean ± SD)	CONT (mean ± SD)	Mean Difference	95% Confidence Interval for Difference		Significance[a]
				Lower Bound	Upper Bound	
Difference Follow-up to Baseline						
∆ R2* Caudate Nucleus	0.12±1.82	-0.17±1.10	0.290	-0.737	1.318	0.527
∆ R2* Pallidum	1.83±4.01	1.03±3.63	0.806	-1.727	3.338	0.525
∆ R2* Putamen	0.51±1.69	0.12±2.09	0.390	-0.758	1.539	0.495
∆ R2* Thalamus	-0.01±1.03	0.53±1.36	0.520	-0.201	1.243	0.153
∆ R2* Substantia nigra	1.71±4.27	0.10±3.83	1.617	-0.989	4.222	0.218
∆ R2* Substantia Nigra Pars Compacta	1.52±4.73	0.69±3.58	0.829	-1.948	3.607	0.551
∆ R2* Substantia Nigra Pars Reticulata	1.65±5.09	0.55±5.99	1.099	-2.297	4.494	0.518

Table 20. Descriptive statistics and t-test of R2* values in PD and control group, difference follow-up to baseline

[a]T-test for independent samples

3.3.2 Cross-sectional Findings

Table 21 shows R2* values in PD and control group, compared by a t-test, at baseline and follow-up examination. R2* values in substantia nigra and its sub regions in PD patients were significantly higher compared to the control group at both times. There was no significant difference between groups in any other region.

Parameter	PD (mean ± SD)	CONT (mean ± SD)	Mean Difference	95% Confidence Interval for Difference		Significance[a]
				Lower Bound	Upper Bound	
Baseline						
R2* Caudate Nucleus	23.40±2.26	23.94±2.32	-0.537	-1.972	0.897	0.455
R2* Pallidum	38.85±5.52	39.40±5.56	-0.556	-4.065	2.954	0.751
R2* Putamen	27.91±3.67	27.80±3.76	0.107	-2.221	2.436	0.937
R2* Thalamus	20.86±1.11	20.93±1.39	-0.069	-0.827	0.690	0.856
R2* Substantia nigra	34.15±4.96	29.27±2.90	4.877	1.154	2.550	**0.000**
R2* Substantia Nigra Pars Compacta	29.89±3.53	25.30±2.67	4.586	2.516	6.655	**0.000**
R2* Substantia Nigra Pars Reticulata	38.12±6.93	32.37±4.49	5.754	2.343	9.164	**0.001**
Follow-up						
R2* Caudate Nucleus	23.52±2.08	23.77±2.49	-0.247	-1.642	1.148	0.723
R2* Pallidum	41.06±6.17	39.84±5.55	1.214	-2.655	5.083	0.531
R2* Putamen	28.42±3.26	27.92±3.05	0.497	-1.518	2.513	0.622
R2* Thalamus	20.85±1.21	20.41±1.42	0.452	-0.353	1.256	0.264
R2* Substantia nigra	35.87±5.26	29.37±3.86	6.494	3.428	9.560	**0.000**
R2* Substantia Nigra Pars Compacta	31.42±4.62	25.99±3.96	5.415	2.627	8.203	**0.000**
R2* Substantia Nigra Pars Reticulata	39.77±6.68	32.92±4.30	6.852	3.050	10.655	**0.001**

Table 21. Descriptive statistics and t-test of R2* values in PD and control group, cross-sectional findings
[a]T-test for independent samples

4 Discussion

The aim of this study was to describe longitudinal evolution of brain iron deposits in PD over a period of two years and compare the findings with non-degenerative tremor syndromes. In the PD group we analysed differences in motor phenotypes and correlated significant changes in brain iron concentration with clinical parameters.

4.1 Methods

4.1.1 MRI-techniques

R2* is an accepted and probably the most popular MRI parameter to estimate brain iron deposits. Many cross-sectional (89-96,99-102,110) as well as all longitudinal studies (114-116) for brain iron deposits in PD used R2*. However R2* does not only reflect iron, but also other local tissue characteristics like difference in water content, brain oxygenation and susceptibility differences other than iron like calcifications (114,131-133). So vascular processes or micro-structural modifications like nigral cell loss might falsify assumed iron concentrations and cover possible significant outcomes. QSM is a superior MRI-technique for quantification of iron deposits and cross-sectional analyses showed significantly higher brain iron deposits in PD using QSM, which R2* could not reveal (77-79,113). To my knowledge there has not been any longitudinal analysis for brain iron in PD using QSM so far, therefore as a next step we will repeat our analysis with QSM-parameters and compare the findings.

4.1.2 ROI-Identification

All ROIs except substantia nigra were automatically segmented from T1 sequences. Substantia nigra and even more its sub-regions have very poor contrast on T1 images which makes direct segmentation impossible. Drawing ROIs for iron quantification on T2 or R2* sequences is problematical, because iron influences contrast and the segmentation may be biased. Moreover exact segmentation is difficult and segmentation normally relies on predetermined shapes which are laid over the MRI scan. Therefore we used a largely iron independent sequence combining normalised R2 and MTR sequences, which

minimises possible biases and enables exact segmentation of the substantia nigra and its subregions.

4.1.3 Clinical examination

Clinical examinations were done in a practical ON-state, which limits the assessment of the progression of PD motor symptoms. Patients showed better results in MDS-UPDRS III (motor examination) and FTM tremor rating scale after the two-year follow-up period, which we interpreted as the effect of treatment optimization. Therefore, the performance of a correlation of changes of iron deposits and the above-mentioned clinical parameters would be inappropriate.

4.2 Results

4.2.1 Longitudinal Analysis in PD

In our PD cohort we found significant R2* increase only in total substantia nigra, whereas significance in the sub regions did not stand correction for multiple comparisons. When correcting for age and sex there were no significant effects in any region.

It is well known that age influences brain iron deposits (134) and it obviously had effects on this current investigation. Persson et al. recently described brain iron deposits in healthy subjects in several RIOs measured by QSM as a function of age and sex. For substantia nigra they found no significant effect of sex on susceptibility evolution going along with normal aging. The age to susceptibility curve for substantia nigra was non-linear with increasing susceptibility until the age of 50, a plateau between 50 and 60 and a slight decline from approximately 60 years of age (135). Based on these results one could speculate that the iron increase in our PD cohort might - at least partly- represent parkinsonian pathology, as the mean age in our PD group was 63.30 ± 10.03 years and one would expect stable or declining iron parameters in the substantia nigra in healthy subjects. From that point of view correction for age and sex is not mandatory and was not performed in similar studies (114-116). Maybe age and sex have higher effects on nigral iron deposits in PD patients than in healthy subjects, which could explain the decline of significance of R2* increase in substantia nigra when correcting for these parameters.

Concerning clinical parameters only LED showed a significant increase when correcting for multiple comparisons. There was a trend for inverse correlation of LED and R2* of global as well as contralateral substantia nigra and its sub-regions with slight significance in global substantia nigra pars reticulata. Considering LED as parameter for disease progression you would expect positive correlation with iron parameters. This contrary trend could indicate a protective effect of levodopa on iron deposits in substantia nigra in PD, however to draw valid conclusions further inquiry will have to be done.

To my knowledge there have been three similar studies done so far, which are summarised in Tables 11-13. Ulla et al. reported increased R2* values in substantia nigra and in the caudal putamen over a period of three years in PD-patients. Moreover they found positive correlation between the variation of R2* and the worsening of PD-motor symptoms (UPDRS III) (114). Wieler et al. performed a three year follow-up study and found significantly increased R2* values in the lateral substantia nigra pars compacta in PD compared to controls at baseline but not at 18 moth or 36 moth follow-up. They also found significant correlation between the R2* change in lateral SNc and the change score in UPDRS III and PDQ-mobility sub score from baseline to 36 month (116). Rossi et al. found increased iron content in a two-year follow-up MRI study in the globus pallidus anterior (significant in T2) as well as slightly in the substantia nigra pars compacta (significant medial SNc in T2). No statistically significant change was found in any region in R2* or SWI (115). In conclusion, considering these and our results there is a trend for longitudinal increase of iron concentration in substantia nigra in PD. As for cross-sectional findings (see Table 10) iron parameters in other brain regions and clinical correlations are quite variable. One reason could be differences in patients' characteristics, for instance disease duration, age, sex, treatment, clinical state at examination-time or grade of clinical affection. Considering the evidence that clinical decline (136,137) and neuro-degeneration (138) in PD as well as normal iron accumulation with age in several brain regions (135) are non-linear processes, comparisons between studies are difficult. On the other hand R2* might not be sensitive enough and differences in MRI protocols and ROI segmentation might explain the different findings. So further studies with higher case-numbers and more sensitive techniques are needed.

Previous cross-sectional studies suggested stronger effects of iron in the substantia nigra only contralateral to the clinically more affected side (84,87,106). Our longitudinal findings partially support this hypothesis. Significances in ANOVAs only considering contralateral R2* values were lower than significances for global values. However mean difference for R2* values in substantia nigra pas compacta was lower than pars reticulata for global ROIs and the other way round for contralateral ROIs. This indicates stronger but less significant effects in the substantia nigra pars compacta only contralateral to the clinically more affected side.

Clinically PD progresses faster in patients with PIGD dominant motor phenotype than in TD patients (27-30). In order to evaluate if this could be due to higher iron concentrations in basal ganglia in PIGD patients, we compared R2* increase in tremor-dominant and non-tremor-dominant PD patients. There was indeed a trend for higher R2* values in PIGD patients in substantia nigra and its sub regions, but no significant differences were found in any global or contralateral ROI. This is in line with previous cross-sectional (109) and longitudinal findings (116). To conclude, there is no significant association between longitudinal R2* increase and PD-motor phenotype.

4.2.2 Comparison with non degenerative tremor syndromes as control group

To my knowledge this is the first analysis comparing cerebral R2* values in different tremor syndromes. For longitudinal evolution repeated measure ANOVAs with group as between-subjects factor as well as t-tests comparing differences did not show significant results for any region. However in substantia nigra there was an obvious trend for higher iron increase in the PD group. The lack of significance may indicate that the study is underpowered and a larger number of subjects is needed. Also, R2* might not be sensitive enough or the observation period of two years is too short to show significant effects.

In cross-sectional comparisons R2* values in substantia nigra and its sub regions were significantly higher in PD compared to the non-degenerative tremor group (essential and dystonic tremor). Neuro-degeneration in substantia nigra is the reason for developing PD, the group-differences in R2* values confirm iron as

important factor in pathogenesis of PD. Moreover considering these results R2* could be a promising non-invasive biomarker in differential diagnosis of tremor syndromes. Nowadays the diagnosis of PD, essential or dystonic tremor mainly relies on clinical examinations. In unclear cases patients have to undergo invasive methods of nuclear medicine (SPECTS or PET) (139). Here R2* could be a cost-effective alternative completely without radio-active tracers and x-ray technology.

4.3 Conclusion

In conclusion R2* increased over a period of two years in the substantia nigra in PD patients. Although the significance was lost after correction for age and sex, we believe that this increase in nigral iron content reflects at least partly worsening of parkinsonian neurodegeneration as previous studies have shown stable or declining iron content in healthy controls in the same age group. Comparison of nigral R2* increase over two years between PD and non-degenerative tremor syndromes revealed no significant differences, but a trend for higher iron increase in PD. Therefore, further studies including more subjects with PD and non-degenerative tremor syndromes and also a group of healthy controls, as well as comparison with more sensitive MRI methods for iron detection such as QSM and longer observation periods are needed. A very interesting novel finding of this study was the significant difference of nigral R2* values between PD and non-degenerative tremor syndromes. This, suggests that R2* might be useful as a diagnostic marker in the differential diagnosis of tremor syndromes.

5 References

(1) Ropper AH, Samuels MA, Klein JP. Parkinson Disease. Adams and Victor's Principles of Neurology. 10th ed.: McGraw-Hill Education; 2014. p. 1082-1095.

(2) von Campenhausen S, Bornschein B, Wick R, Botzel K, Sampaio C, Poewe W, et al. Prevalence and incidence of Parkinson's disease in Europe. Eur Neuropsychopharmacol 2005 Aug;15(4):473-490.

(3) Pringsheim T, Jette N, Frolkis A, Steeves TDL. The prevalence of Parkinson's disease: A systematic review and meta-analysis. Movement Disorders 2014;29(13):1583-1590.

(4) Wenning GK, Kiechl S, Seppi K, Muller J, Hogl B, Saletu M, et al. Prevalence of movement disorders in men and women aged 50-89 years (Bruneck Study cohort): a population-based study. Lancet Neurol 2005 Dec;4(12):815-820.

(5) Braak H, Del Tredici K. Invited Article: Nervous system pathology in sporadic Parkinson disease. Neurology 2008 May 13;70(20):1916-1925.

(6) Brice A. Genetics of Parkinson's disease: LRRK2 on the rise. Brain 2005 Dec;128(Pt 12):2760-2762.

(7) Eriksen JL, Dawson TM, Dickson DW, Petrucelli L. Caught in the act: alpha-synuclein is the culprit in Parkinson's disease. Neuron 2003 Oct 30;40(3):453-456.

(8) Lees AJ. Trauma and Parkinson disease. Rev Neurol (Paris) 1997 Oct;153(10):541-546.

(9) Lohmann E, Periquet M, Bonifati V, Wood NW, De Michele G, Bonnet AM, et al. How much phenotypic variation can be attributed to parkin genotype? Ann Neurol 2003 Aug;54(2):176-185.

(10) Pakkenberg B, Moller A, Gundersen HJ, Mouritzen Dam A, Pakkenberg H. The absolute number of nerve cells in substantia nigra in normal subjects and in patients with Parkinson's disease estimated with an unbiased stereological method. J Neurol Neurosurg Psychiatry 1991 Jan;54(1):30-33.

(11) Piccini P, Burn DJ, Ceravolo R, Maraganore D, Brooks DJ. The role of inheritance in sporadic Parkinson's disease: evidence from a longitudinal study of dopaminergic function in twins. Ann Neurol 1999 May;45(5):577-582.

(12) Polymeropoulos MH, Lavedan C, Leroy E, Ide SE, Dehejia A, Dutra A, et al. Mutation in the alpha-synuclein gene identified in families with Parkinson's disease. Science 1997 Jun 27;276(5321):2045-2047.

(13) Sidransky E, Nalls MA, Aasly JO, Aharon-Peretz J, Annesi G, Barbosa ER, et al. Multicenter analysis of glucocerebrosidase mutations in Parkinson's disease. N Engl J Med 2009 Oct 22;361(17):1651-1661.

(14) Singleton AB, Farrer M, Johnson J, Singleton A, Hague S, Kachergus J, et al. alpha-Synuclein locus triplication causes Parkinson's disease. Science 2003 Oct 31;302(5646):841.

(15) Snyder SH, D'Amato RJ. MPTP: a neurotoxin relevant to the pathophysiology of Parkinson's disease. The 1985 George C. Cotzias lecture. Neurology 1986 Feb;36(2):250-258.

(16) Uhl GR, Javitch JA, Snyder SH. Normal MPTP binding in parkinsonian substantial nigra: evidence for extraneuronal toxin conversion in human brain. Lancet 1985 Apr 27;1(8435):956-957.

(17) Valente EM, Abou-Sleiman PM, Caputo V, Muqit MM, Harvey K, Gispert S, et al. Hereditary early-onset Parkinson's disease caused by mutations in PINK1. Science 2004 May 21;304(5674):1158-1160.

(18) Ropper AH, Samuels MA, Klein JP. Abnormalities of Movement and Posture Caused by Disease of the Basal Ganglia. Adams and Victor's Principles of Neurology. 10th ed.: McGraw-Hill Education; 2014. p. 64-80.

(19) Ropper AH, Samuels MA, Klein JP. Tremor, Myolonus, Focal Dystonias, and tics. Adams and Victor's Principles of Neurology. 10th ed.: McGraw-Hill Education; 2014. p. 92-114.

(20) Hoehn MM, Yahr MD. Parkinsonism: onset, progression, and mortality. 1967. Neurology 2001 Nov;57(10 Suppl 3):S11-26.

(21) Poewe W. Clinical measures of progression in Parkinson's disease. Mov Disord 2009;24 Suppl 2:S671-6.

(22) Zhou MZ, Gan J, Wei YR, Ren XY, Chen W, Liu ZG. The association between non-motor symptoms in Parkinson's disease and age at onset. Clin Neurol Neurosurg 2013 Oct;115(10):2103-2107.

(23) Aarsland D, Zaccai J, Brayne C. A systematic review of prevalence studies of dementia in Parkinson's disease. Mov Disord 2005 Oct;20(10):1255-1263.

(24) Martinez-Martin P, Chaudhuri KR, Rojo-Abuin JM, Rodriguez-Blazquez C, Alvarez-Sanchez M, Arakaki T, et al. Assessing the non-motor symptoms of Parkinson's disease: MDS-UPDRS and NMS Scale. Eur J Neurol 2015 Jan;22(1):37-43.

(25) Hughes AJ, Daniel SE, Kilford L, Lees AJ. Accuracy of clinical diagnosis of idiopathic Parkinson's disease: a clinico-pathological study of 100 cases. J Neurol Neurosurg Psychiatry 1992 Mar;55(3):181-184.

(26) Goetz CG, Tilley BC, Shaftman SR, Stebbins GT, Fahn S, Martinez-Martin P, et al. Movement Disorder Society-sponsored revision of the Unified Parkinson's Disease Rating Scale (MDS-UPDRS): scale presentation and clinimetric testing results. Mov Disord 2008 Nov 15;23(15):2129-2170.

(27) Xia R, Mao ZH. Progression of motor symptoms in Parkinson's disease. Neurosci Bull 2012 Feb;28(1):39-48.

(28) Louis ED, Tang MX, Cote L, Alfaro B, Mejia H, Marder K. Progression of parkinsonian signs in Parkinson disease. Arch Neurol 1999 Mar;56(3):334-337.

(29) Schupbach WM, Corvol JC, Czernecki V, Djebara MB, Golmard JL, Agid Y, et al. Segmental progression of early untreated Parkinson's disease: a novel approach to clinical rating. J Neurol Neurosurg Psychiatry 2010 Jan;81(1):20-25.

(30) Vu TC, Nutt JG, Holford NH. Progression of motor and nonmotor features of Parkinson's disease and their response to treatment. Br J Clin Pharmacol 2012 Aug;74(2):267-283.

(31) Erro R, Picillo M, Vitale C, Amboni M, Moccia M, Longo K, et al. Non-motor symptoms in early Parkinson's disease: a 2-year follow-up study on previously untreated patients. J Neurol Neurosurg Psychiatry 2013 Jan;84(1):14-17.

(32) Hely MA, Morris JG, Reid WG, Trafficante R. Sydney Multicenter Study of Parkinson's disease: non-L-dopa-responsive problems dominate at 15 years. Mov Disord 2005 Feb;20(2):190-199.

(33) Hely MA, Reid WG, Adena MA, Halliday GM, Morris JG. The Sydney multicenter study of Parkinson's disease: the inevitability of dementia at 20 years. Mov Disord 2008 Apr 30;23(6):837-844.

(34) Gotz ME, Double K, Gerlach M, Youdim MB, Riederer P. The relevance of iron in the pathogenesis of Parkinson's disease. Ann N Y Acad Sci 2004 Mar;1012:193-208.

(35) Zecca L, Youdim MB, Riederer P, Connor JR, Crichton RR. Iron, brain ageing and neurodegenerative disorders. Nat Rev Neurosci 2004 Nov;5(11):863-873.

(36) Crichton RR, Dexter DT, Ward RJ. Brain iron metabolism and its perturbation in neurological diseases. J Neural Transm (Vienna) 2011 Mar;118(3):301-314.

(37) Zucca FA, Segura-Aguilar J, Ferrari E, Munoz P, Paris I, Sulzer D, et al. Interactions of iron, dopamine and neuromelanin pathways in brain aging and Parkinson's disease. Prog Neurobiol 2015 Oct 9.

(38) Sian-Hulsmann J, Mandel S, Youdim MB, Riederer P. The relevance of iron in the pathogenesis of Parkinson's disease. J Neurochem 2011 Sep;118(6):939-957.

(39) Brass SD, Chen NK, Mulkern RV, Bakshi R. Magnetic resonance imaging of iron deposition in neurological disorders. Top Magn Reson Imaging 2006 Feb;17(1):31-40.

(40) Mochizuki H, Yasuda T. Iron accumulation in Parkinson's disease. J Neural Transm (Vienna) 2012 Dec;119(12):1511-1514.

(41) Mariani S, Ventriglia M, Simonelli I, Donno S, Bucossi S, Vernieri F, et al. Fe and Cu do not differ in Parkinson's disease: a replication study plus meta-analysis. Neurobiol Aging 2013 Feb;34(2):632-633.

(42) Madenci G, Bilen S, Arli B, Saka M, Ak F. Serum iron, vitamin B12 and folic acid levels in Parkinson's disease. Neurochem Res 2012 Jul;37(7):1436-1441.

(43) Farhoudi M, Taheraghdam A, Farid GA, Talebi M, Pashapou A, Majidi J, et al. Serum iron and ferritin level in idiopathic Parkinson. Pak J Biol Sci 2012 Nov 15;15(22):1094-1097.

(44) Pichler I, Del Greco MF, Gogele M, Lill CM, Bertram L, Do CB, et al. Serum iron levels and the risk of Parkinson disease: a Mendelian randomization study. PLoS Med 2013;10(6):e1001462.

(45) Ward RJ, Zucca FA, Duyn JH, Crichton RR, Zecca L. The role of iron in brain ageing and neurodegenerative disorders. Lancet Neurol 2014 Oct;13(10):1045-1060.

(46) Lhermitte J, Kraus WM, McAlpine D. Original Papers: ON THE OCCURRENCE OF ABNORMAL DEPOSITS OF IRON IN THE BRAIN IN PARKINSONISM WITH SPECIAL REFERENCE TO ITS LOCALISATION. J Neurol Psychopathol 1924 Nov;5(19):195-208.

(47) Earle KM. Studies on Parkinson's disease including x-ray fluorescent spectroscopy of formalin fixed brain tissue. J Neuropathol Exp Neurol 1968 Jan;27(1):1-14.

(48) Jellinger K, Kienzl E, Rumpelmair G, Riederer P, Stachelberger H, Ben-Shachar D, et al. Iron-melanin complex in substantia nigra of parkinsonian brains: an x-ray microanalysis. J Neurochem 1992 Sep;59(3):1168-1171.

(49) Riederer P, Sofic E, Rausch WD, Schmidt B, Reynolds GP, Jellinger K, et al. Transition metals, ferritin, glutathione, and ascorbic acid in parkinsonian brains. J Neurochem 1989 Feb;52(2):515-520.

(50) Dexter DT, Carayon A, Javoy-Agid F, Agid Y, Wells FR, Daniel SE, et al. Alterations in the levels of iron, ferritin and other trace metals in Parkinson's disease and other neurodegenerative diseases affecting the basal ganglia. Brain 1991 Aug;114 (Pt 4)(Pt 4):1953-1975.

(51) Dexter DT, Wells FR, Lees AJ, Agid F, Agid Y, Jenner P, et al. Increased nigral iron content and alterations in other metal ions occurring in brain in Parkinson's disease. J Neurochem 1989 Jun;52(6):1830-1836.

(52) Dexter DT, Carayon A, Vidailhet M, Ruberg M, Agid F, Agid Y, et al. Decreased ferritin levels in brain in Parkinson's disease. J Neurochem 1990 Jul;55(1):16-20.

(53) Good PF, Olanow CW, Perl DP. Neuromelanin-containing neurons of the substantia nigra accumulate iron and aluminum in Parkinson's disease: a LAMMA study. Brain Res 1992 Oct 16;593(2):343-346.

(54) Griffiths PD, Dobson BR, Jones GR, Clarke DT. Iron in the basal ganglia in Parkinson's disease. An in vitro study using extended X-ray absorption fine structure and cryo-electron microscopy. Brain 1999 Apr;122 (Pt 4)(Pt 4):667-673.

(55) Uitti RJ, Rajput AH, Rozdilsky B, Bickis M, Wollin T, Yuen WK. Regional metal concentrations in Parkinson's disease, other chronic neurological diseases, and control brains. Can J Neurol Sci 1989 Aug;16(3):310-314.

(56) Loeffler DA, Connor JR, Juneau PL, Snyder BS, Kanaley L, DeMaggio AJ, et al. Transferrin and iron in normal, Alzheimer's disease, and Parkinson's disease brain regions. J Neurochem 1995 Aug;65(2):710-724.

(57) Galazka-Friedman J, Bauminger ER, Friedman A, Barcikowska M, Hechel D, Nowik I. Iron in parkinsonian and control substantia nigra--a Mossbauer spectroscopy study. Mov Disord 1996 Jan;11(1):8-16.

(58) Sofic E, Riederer P, Heinsen H, Beckmann H, Reynolds GP, Hebenstreit G, et al. Increased iron (III) and total iron content in post mortem substantia nigra of parkinsonian brain. J Neural Transm 1988;74(3):199-205.

(59) Sofic E, Paulus W, Jellinger K, Riederer P, Youdim MB. Selective increase of iron in substantia nigra zona compacta of parkinsonian brains. J Neurochem 1991 Mar;56(3):978-982.

(60) Hirsch EC, Brandel JP, Galle P, Javoy-Agid F, Agid Y. Iron and aluminum increase in the substantia nigra of patients with Parkinson's disease: an X-ray microanalysis. J Neurochem 1991 Feb;56(2):446-451.

(61) Groger A, Berg D. Does structural neuroimaging reveal a disturbance of iron metabolism in Parkinson's disease? Implications from MRI and TCS studies. J Neural Transm (Vienna) 2012 Dec;119(12):1523-1528.

(62) Sprawls P. Magnetic resonance Imaging: Principles, Methods, and Techniques;Online Edition. Available at: http://www.sprawls.org/mripmt/index.html. Accessed 02/13, 2016.

(63) Schenck JF. Magnetic resonance imaging of brain iron. J Neurol Sci 2003 Mar 15;207(1-2):99-102.

(64) Haacke EM, Cheng NY, House MJ, Liu Q, Neelavalli J, Ogg RJ, et al. Imaging iron stores in the brain using magnetic resonance imaging. Magn Reson Imaging 2005 Jan;23(1):1-25.

(65) Schenck JF, Zimmerman EA. High-field magnetic resonance imaging of brain iron: birth of a biomarker? NMR Biomed 2004 Nov;17(7):433-445.

(66) Michaeli S, Oz G, Sorce DJ, Garwood M, Ugurbil K, Majestic S, et al. Assessment of brain iron and neuronal integrity in patients with Parkinson's disease using novel MRI contrasts. Mov Disord 2007 Feb 15;22(3):334-340.

(67) Nestrasil I, Michaeli S, Liimatainen T, Rydeen CE, Kotz CM, Nixon JP, et al. T1rho and T2rho MRI in the evaluation of Parkinson's disease. J Neurol 2010 Jun;257(6):964-968.

(68) Haacke EM, Xu Y, Cheng YC, Reichenbach JR. Susceptibility weighted imaging (SWI). Magn Reson Med 2004 Sep;52(3):612-618.

(69) Gasparotti R, Pinelli L, Liserre R. New MR sequences in daily practice: susceptibility weighted imaging. A pictorial essay. Insights Imaging 2011 Jun;2(3):335-347.

(70) Ogg RJ, Langston JW, Haacke EM, Steen RG, Taylor JS. The correlation between phase shifts in gradient-echo MR images and regional brain iron concentration. Magn Reson Imaging 1999 Oct;17(8):1141-1148.

(71) Haacke EM, Mittal S, Wu Z, Neelavalli J, Cheng YC. Susceptibility-weighted imaging: technical aspects and clinical applications, part 1. AJNR Am J Neuroradiol 2009 Jan;30(1):19-30.

(72) Liu C, Li W, Tong KA, Yeom KW, Kuzminski S. Susceptibility-weighted imaging and quantitative susceptibility mapping in the brain. J Magn Reson Imaging 2015 Jul;42(1):23-41.

(73) Wang Y, Liu T. Quantitative susceptibility mapping (QSM): Decoding MRI data for a tissue magnetic biomarker. Magn Reson Med 2015 Jan;73(1):82-101.

(74) Liu T, Spincemaille P, de Rochefort L, Kressler B, Wang Y. Calculation of susceptibility through multiple orientation sampling (COSMOS): a method for conditioning the inverse problem from measured magnetic field map to susceptibility source image in MRI. Magn Reson Med 2009 Jan;61(1):196-204.

(75) Haacke EM, Liu S, Buch S, Zheng W, Wu D, Ye Y. Quantitative susceptibility mapping: current status and future directions. Magn Reson Imaging 2015 Jan;33(1):1-25.

(76) Langkammer C, Schweser F, Krebs N, Deistung A, Goessler W, Scheurer E, et al. Quantitative susceptibility mapping (QSM) as a means to measure brain iron? A post mortem validation study. Neuroimage 2012 Sep;62(3):1593-1599.

(77) Murakami Y, Kakeda S, Watanabe K, Ueda I, Ogasawara A, Moriya J, et al. Usefulness of quantitative susceptibility mapping for the diagnosis of Parkinson disease. AJNR Am J Neuroradiol 2015 Jun;36(6):1102-1108.

(78) Barbosa JH, Santos AC, Tumas V, Liu M, Zheng W, Haacke EM, et al. Quantifying brain iron deposition in patients with Parkinson's disease using quantitative susceptibility mapping, R2 and R2. Magn Reson Imaging 2015 Jun;33(5):559-565.

(79) Du G, Liu T, Lewis MM, Kong L, Wang Y, Connor J, et al. Quantitative susceptibility mapping of the midbrain in Parkinson's disease. Mov Disord 2015 Sep 12.

(80) Antonini A, Leenders KL, Meier D, Oertel WH, Boesiger P, Anliker M. T2 relaxation time in patients with Parkinson's disease. Neurology 1993 Apr;43(4):697-700.

(81) Vymazal J, Righini A, Brooks RA, Canesi M, Mariani C, Leonardi M, et al. T1 and T2 in the brain of healthy subjects, patients with Parkinson disease, and patients with multiple system atrophy: relation to iron content. Radiology 1999 May;211(2):489-495.

(82) Mondino F, Filippi P, Magliola U, Duca S. Magnetic resonance relaxometry in Parkinson's disease. Neurol Sci 2002 Sep;23 Suppl 2:S87-8.

(83) Atasoy HT, Nuyan O, Tunc T, Yorubulut M, Unal AE, Inan LE. T2-weighted MRI in Parkinson's disease; substantia nigra pars compacta hypointensity correlates with the clinical scores. Neurol India 2004 Sep;52(3):332-337.

(84) Kosta P, Argyropoulou MI, Markoula S, Konitsiotis S. MRI evaluation of the basal ganglia size and iron content in patients with Parkinson's disease. J Neurol 2006 Jan;253(1):26-32.

(85) Brar S, Henderson D, Schenck J, Zimmerman EA. Iron accumulation in the substantia nigra of patients with Alzheimer disease and parkinsonism. Arch Neurol 2009 Mar;66(3):371-374.

(86) Ye FQ, Allen PS, Martin WR. Basal ganglia iron content in Parkinson's disease measured with magnetic resonance. Mov Disord 1996 May;11(3):243-249.

(87) Wallis LI, Paley MN, Graham JM, Grunewald RA, Wignall EL, Joy HM, et al. MRI assessment of basal ganglia iron deposition in Parkinson's disease. J Magn Reson Imaging 2008 Nov;28(5):1061-1067.

(88) Boelmans K, Holst B, Hackius M, Finsterbusch J, Gerloff C, Fiehler J, et al. Brain iron deposition fingerprints in Parkinson's disease and progressive supranuclear palsy. Mov Disord 2012 Mar;27(3):421-427.

(89) Gorell JM, Ordidge RJ, Brown GG, Deniau JC, Buderer NM, Helpern JA. Increased iron-related MRI contrast in the substantia nigra in Parkinson's disease. Neurology 1995 Jun;45(6):1138-1143.

(90) Graham JM, Paley MN, Grunewald RA, Hoggard N, Griffiths PD. Brain iron deposition in Parkinson's disease imaged using the PRIME magnetic resonance sequence. Brain 2000 Dec;123 Pt 12:2423-2431.

(91) Ryvlin P, Broussolle E, Piollet H, Viallet F, Khalfallah Y, Chazot G. Magnetic resonance imaging evidence of decreased putamenal iron content in idiopathic Parkinson's disease. Arch Neurol 1995 Jun;52(6):583-588.

(92) Baudrexel S, Nurnberger L, Rub U, Seifried C, Klein JC, Deller T, et al. Quantitative mapping of T1 and T2* discloses nigral and brainstem pathology in early Parkinson's disease. Neuroimage 2010 Jun;51(2):512-520.

(93) Peran P, Cherubini A, Assogna F, Piras F, Quattrocchi C, Peppe A, et al. Magnetic resonance imaging markers of Parkinson's disease nigrostriatal signature. Brain 2010 Nov;133(11):3423-3433.

(94) Du G, Lewis MM, Styner M, Shaffer ML, Sen S, Yang QX, et al. Combined R2* and diffusion tensor imaging changes in the substantia nigra in Parkinson's disease. Mov Disord 2011 Aug 1;26(9):1627-1632.

(95) Du G, Lewis MM, Shaffer ML, Chen H, Yang QX, Mailman RB, et al. Serum cholesterol and nigrostriatal R2* values in Parkinson's disease. PLoS One 2012;7(4):e35397.

(96) Bunzeck N, Singh-Curry V, Eckart C, Weiskopf N, Perry RJ, Bain PG, et al. Motor phenotype and magnetic resonance measures of basal ganglia iron levels in Parkinson's disease. Parkinsonism Relat Disord 2013 Dec;19(12):1136-1142.

(97) Wang C, Fan G, Xu K, Wang S. Quantitative assessment of iron deposition in the midbrain using 3D-enhanced T2 star weighted angiography (ESWAN): a preliminary cross-sectional study of 20 Parkinson's disease patients. Magn Reson Imaging 2013 Sep;31(7):1068-1073.

(98) Lewis MM, Du G, Kidacki M, Patel N, Shaffer ML, Mailman RB, et al. Higher iron in the red nucleus marks Parkinson's dyskinesia. Neurobiol Aging 2013 May;34(5):1497-1503.

(99) Aquino D, Contarino V, Albanese A, Minati L, Farina L, Grisoli M, et al. Substantia nigra in Parkinson's disease: a multimodal MRI comparison between early and advanced stages of the disease. Neurol Sci 2014 May;35(5):753-758.

(100) Virel A, Faergemann E, Oradd G, Stromberg I. Magnetic resonance imaging (MRI) to study striatal iron accumulation in a rat model of Parkinson's disease. PLoS One 2014 Nov 14;9(11):e112941.

(101) Pyatigorskaya N, Sharman M, Corvol JC, Valabregue R, Yahia-Cherif L, Poupon F, et al. High nigral iron deposition in LRRK2 and Parkin mutation carriers using R2* relaxometry. Mov Disord 2015 Jul;30(8):1077-1084.

(102) Reimao S, Ferreira S, Nunes RG, Pita Lobo P, Neutel D, Abreu D, et al. Magnetic resonance correlation of iron content with neuromelanin in the substantia nigra of early-stage Parkinson's disease. Eur J Neurol 2016 Feb;23(2):368-374.

(103) Bartzokis G, Cummings JL, Markham CH, Marmarelis PZ, Treciokas LJ, Tishler TA, et al. MRI evaluation of brain iron in earlier- and later-onset Parkinson's disease and normal subjects. Magn Reson Imaging 1999 Feb;17(2):213-222.

(104) Bartzokis G, Tishler TA, Shin IS, Lu PH, Cummings JL. Brain ferritin iron as a risk factor for age at onset in neurodegenerative diseases. Ann N Y Acad Sci 2004 Mar;1012:224-236.

(105) Zhang W, Sun SG, Jiang YH, Qiao X, Sun X, Wu Y. Determination of brain iron content in patients with Parkinson's disease using magnetic susceptibility imaging. Neurosci Bull 2009 Dec;25(6):353-360.

(106) Zhang J, Zhang Y, Wang J, Cai P, Luo C, Qian Z, et al. Characterizing iron deposition in Parkinson's disease using susceptibility-weighted imaging: an in vivo MR study. Brain Res 2010 May 12;1330:124-130.

(107) Huang XM, Sun B, Xue YJ, Duan Q. Susceptibility-weighted imaging in detecting brain iron accumulation of Parkinson's disease. Zhonghua Yi Xue Za Zhi 2010 Nov 23;90(43):3054-3058.

(108) Lotfipour AK, Wharton S, Schwarz ST, Gontu V, Schafer A, Peters AM, et al. High resolution magnetic susceptibility mapping of the substantia nigra in Parkinson's disease. J Magn Reson Imaging 2012 Jan;35(1):48-55.

(109) Jin L, Wang J, Jin H, Fei G, Zhang Y, Chen W, et al. Nigral iron deposition occurs across motor phenotypes of Parkinson's disease. Eur J Neurol 2012 Jul;19(7):969-976.

(110) Wang Y, Butros SR, Shuai X, Dai Y, Chen C, Liu M, et al. Different iron-deposition patterns of multiple system atrophy with predominant parkinsonism and idiopathetic Parkinson diseases demonstrated by phase-corrected susceptibility-weighted imaging. AJNR Am J Neuroradiol 2012 Feb;33(2):266-273.

(111) Rossi M, Ruottinen H, Soimakallio S, Elovaara I, Dastidar P. Clinical MRI for iron detection in Parkinson's disease. Clin Imaging 2013 Jul-Aug;37(4):631-636.

(112) Wu SF, Zhu ZF, Kong Y, Zhang HP, Zhou GQ, Jiang QT, et al. Assessment of cerebral iron content in patients with Parkinson's disease by the susceptibility-weighted MRI. Eur Rev Med Pharmacol Sci 2014;18(18):2605-2608.

(113) He N, Ling H, Ding B, Huang J, Zhang Y, Zhang Z, et al. Region-specific disturbed iron distribution in early idiopathic Parkinson's disease measured by quantitative susceptibility mapping. Hum Brain Mapp 2015 Nov;36(11):4407-4420.

(114) Ulla M, Bonny JM, Ouchchane L, Rieu I, Claise B, Durif F. Is R2* a new MRI biomarker for the progression of Parkinson's disease? A longitudinal follow-up. PLoS One 2013;8(3):e57904.

(115) Rossi ME, Ruottinen H, Saunamaki T, Elovaara I, Dastidar P. Imaging brain iron and diffusion patterns: a follow-up study of Parkinson's disease in the initial stages. Acad Radiol 2014 Jan;21(1):64-71.

(116) Wieler M, Gee M, Martin WR. Longitudinal midbrain changes in early Parkinson's disease: iron content estimated from R2*/MRI. Parkinsonism Relat Disord 2015 Mar;21(3):179-183.

(117) Wieler M, Gee M, Camicioli R, Martin WR. Freezing of gait in early Parkinson's disease: Nigral iron content estimated from magnetic resonance imaging. J Neurol Sci 2016 Feb 15;361:87-91.

(118) Stebbins GT, Goetz CG, Burn DJ, Jankovic J, Khoo TK, Tilley BC. How to identify tremor dominant and postural instability/gait difficulty groups with the movement disorder society unified Parkinson's disease rating scale: comparison with the unified Parkinson's disease rating scale. Mov Disord 2013 May;28(5):668-670.

(119) Yoo K, Chung SJ, Kim HS, Choung OH, Lee YB, Kim MJ, et al. Neural substrates of motor and non-motor symptoms in Parkinson's disease: a resting FMRI study. PLoS One 2015 Apr 24;10(4):e0125455.

(120) Fahn S, Tolosa E, Concepcion M. Clinical Rating Scale for Tremor. In: Jankovic J TE, editor. Parkinson’s disease and movement disorders. 2nd ed. Baltimore: Williams and Wilkins; 1993. p. 271-280.

(121) Stacy MA, Elble RJ, Ondo WG, Wu SC, Hulihan J, TRS study group. Assessment of interrater and intrarater reliability of the Fahn-Tolosa-Marin Tremor Rating Scale in essential tremor. Mov Disord 2007 Apr 30;22(6):833-838.

(122) Chaudhuri KR, Martinez-Martin P, Schapira AH, Stocchi F, Sethi K, Odin P, et al. International multicenter pilot study of the first comprehensive self-completed nonmotor symptoms questionnaire for Parkinson's disease: the NMSQuest study. Mov Disord 2006 Jul;21(7):916-923.

(123) Chaudhuri KR, Martinez-Martin P, Brown RG, Sethi K, Stocchi F, Odin P, et al. The metric properties of a novel non-motor symptoms scale for Parkinson's disease: Results from an international pilot study. Mov Disord 2007 Oct 15;22(13):1901-1911.

(124) Tomlinson CL, Stowe R, Patel S, Rick C, Gray R, Clarke CE. Systematic review of levodopa dose equivalency reporting in Parkinson's disease. Mov Disord 2010 Nov 15;25(15):2649-2653.

(125) Morris JC, Heyman A, Mohs RC, Hughes JP, van Belle G, Fillenbaum G, et al. The Consortium to Establish a Registry for Alzheimer's Disease (CERAD). Part I. Clinical and neuropsychological assessment of Alzheimer's disease. Neurology 1989 Sep;39(9):1159-1165.

(126) Chandler MJ, Lacritz LH, Hynan LS, Barnard HD, Allen G, Deschner M, et al. A total score for the CERAD neuropsychological battery. Neurology 2005 Jul 12;65(1):102-106.

(127) Seo EH, Lee DY, Lee JH, Choo IH, Kim JW, Kim SG, et al. Total scores of the CERAD neuropsychological assessment battery: validation for mild cognitive impairment and dementia patients with diverse etiologies. Am J Geriatr Psychiatry 2010 Sep;18(9):801-809.

(128) Paajanen T, Hanninen T, Tunnard C, Hallikainen M, Mecocci P, Sobow T, et al. CERAD neuropsychological compound scores are accurate in detecting prodromal alzheimer's disease: a prospective AddNeuroMed study. J Alzheimers Dis 2014;39(3):679-690.

(129) Schweser F, Deistung A, Lehr BW, Reichenbach JR. Quantitative imaging of intrinsic magnetic tissue properties using MRI signal phase: an approach to in vivo brain iron metabolism? Neuroimage 2011 Feb 14;54(4):2789-2807.

(130) Zollei L, Stevens A, Huber K, Kakunoori S, Fischl B. Improved tractography alignment using combined volumetric and surface registration. Neuroimage 2010 May 15;51(1):206-213.

(131) Yablonskiy DA, Haacke EM. Theory of NMR signal behavior in magnetically inhomogeneous tissues: the static dephasing regime. Magn Reson Med 1994 Dec;32(6):749-763.

(132) Punwani S, Cooper CE, Clemence M, Penrice J, Amess P, Thornton J, et al. Correlation between absolute deoxyhaemoglobin [dHb] measured by near infrared spectroscopy (NIRS) and absolute R2' as determined by magnetic resonance imaging (MRI). Adv Exp Med Biol 1997;413:129-137.

(133) Mitsumori F, Watanabe H, Takaya N. Estimation of brain iron concentration in vivo using a linear relationship between regional iron and apparent transverse relaxation rate of the tissue water at 4.7T. Magn Reson Med 2009 Nov;62(5):1326-1330.

(134) HALLGREN B, SOURANDER P. The effect of age on the non-haemin iron in the human brain. J Neurochem 1958 Oct;3(1):41-51.

(135) Persson N, Wu J, Zhang Q, Liu T, Shen J, Bao R, et al. Age and sex related differences in subcortical brain iron concentrations among healthy adults. Neuroimage 2015 Nov 15;122:385-398.

(136) Hindle JV. Ageing, neurodegeneration and Parkinson’s disease. Age and Ageing 2010 March 01;39(2):156-161.

(137) Kempster PA, Williams DR, Selikhova M, Holton J, Revesz T, Lees AJ. Patterns of levodopa response in Parkinson's disease: a clinico-pathological study. Brain 2007 Aug;130(Pt 8):2123-2128.

(138) Braak H, Ghebremedhin E, Rub U, Bratzke H, Del Tredici K. Stages in the development of Parkinson's disease-related pathology. Cell Tissue Res 2004 Oct;318(1):121-134.

(139) Botzel K, Tronnier V, Gasser T. The differential diagnosis and treatment of tremor. Dtsch Arztebl Int 2014 Mar 28;111(13):225-35; quiz 236.

(140) Silbernagl S, Lang F. Erkrankungen der Basalganglien. Taschenatlas Pathophysiologie. 3rd ed.: Georg Thieme Verlag; 2009. p. 334-337.